J|A|C|S
ARTICLES
Published on Web 04/28/2004

Atropisomerization, C−H Activation, and Dissociative Substitution at Some Biphenyl Platinum(II) Complexes

Maria Rosaria Plutino,[‡] Luigi Monsu' Scolaro,[†,§] Alberto Albinati,[||] and Raffaello Romeo*[,†]

Contribution from the Dipartimento di Chimica Inorganica, Chimica Analitica e Chimica Fisica, Università di Messina − Salita Sperone, 31 − Vill. S. Agata − 98166 Messina, Italy, ISMN − CNR, Sezione di Palermo, Unità di Messina, INFM, Unità di Messina, and Dipartimento di Chimica Strutturale e Stereochimica Inorganica, Facoltà di Farmacia, Università di Milano, 20133 Milano, Italy

Received August 7, 2003; E-mail: raf.romeo@chem.unime.it

Abstract: The reaction of 2,2′-dilithiumbiphenyl with *cis*-[$PtCl_2(SEt_2)_2$] at −10 °C in diethyl ether not only leads to the main product [$Pt_2(\mu\text{-}SEt_2)_2(bph)_2$], containing the planar 2,2′-biphenyl dianion (bph^{2-}), but also forms a new dinuclear platinum(II) compound of formula [$Pt_2(\mu\text{-}SEt_2)_2(Hbph)_4$], **1a** ($Hbph^- = \eta^1$-biphenyl monoanion), in which each metal is in a square-planar environment. NMR spectroscopy and molecular mechanics (MMFF) calculations were used to characterize **1a**. The results suggest that the favored conformation for the four Hbph biphenyl groups is $\alpha\beta\beta\alpha$. In chloroform solution, **1a** undergoes atropisomerization to **1b** ($\alpha\beta\alpha\beta$) ($k_{is} = 1.03 \times 10^{-4}$ s^{-1}, at 298 K) that subsequently cyclometalates ($k_{obs} = 4.48 \times 10^{-6}$ s^{-1}, at 298 K) to yield [$Pt_2(\mu\text{-}SEt_2)_2(bph)_2$] and biphenyl. Both processes, atropisomerization and C−H activation, presumably involve preliminary thioether bridge splitting. The dinuclear complex **1a** has been shown to be a versatile and useful precursor to a variety of mononuclear η^1-biphenyl platinum(II) complexes. By reaction with diethyl sulfide, dimethyl sulfoxide, or with rigid dinitrogen containing ligands, such as 2,2′-bipyridine or 1,10-phenanthroline, complexes *cis*-[$Pt(Hbph)_2(dmso)_2$] **3**, *cis*-[$Pt(Hbph)_2(SEt_2)_2$] **4**, [$Pt(Hbph)_2(bpy)$] **5**, and [$Pt(Hbph)_2(phen)$] **6** were obtained, respectively. The crystal structures of compounds **5** and **6** were determined. Only the head-to-tail isomer of these compounds was recognized in the solid state and in solution, where restricted rotation around the Pt−C bond prevents interconversion to the head-to-head form. A detailed kinetic study of ligand (dmso) exchange and substitution (by 2,2′-bipyridine and 1,10-phenanthroline) has been performed on complex **3** in $CDCl_3$ and toluene-d_8 by ^{1}H NMR magnetization transfer experiments, and in toluene by UV/vis spectroscopy, respectively. The rates of both processes show no dependence on ligand concentration, the rate of ligand substitution being in reasonable agreement with that of ligand exchange at the same temperature. The kinetics are characterized by largely positive entropies of activation. The results are consistent with a dissociative mode of activation analogous to the pattern already found for compounds with a similar [Pt(C,C)(S,S)] set of coordinating ligands. The role of ML_3 d^8 T-shaped 14-electron species, as elusive reaction intermediates or structurally characterized compounds, is discussed.

Introduction

A rational design of square-planar platinum(II) compounds with specific therapeutic properties requires a deep knowledge of their substitution behavior, because it is necessary to predict what happens along the way to the biological target and what the reactivity will be in a biological environment.[1] Thus, following Rosenberg's discovery of the antitumor properties of *cis*-platin,[2] studies on substitution reactions of Pt(II) complexes have received an increasing renewal of interest. The mechanistic picture currently appears to be reasonably clear, and it involves the direct attack of a nucleophile on the substrate with formation of a transient five-coordinate intermediate.[3] Old concepts have been revisited, such as the trans and cis effects in their σ and π components,[4] steric effects, nucleophilic and nucleofuge abilities

[†] Dipartimento di Chimica Inorganica, Università di Messina.
[‡] ISMN − CNR, Unità di Messina.
[§] INFM, Unità di Messina.
[||] Università di Milano.

(1) *Cisplatin: Chemistry and Biochemistry of a Leading Anticancer Drug*; Lippert, B., Ed.; Wiley-VCH: Weinheim, 1999.
(2) Rosenberg, B.; Van Camp, L.; Trosko, J. E.; Mansour, V. H. *Nature* **1969**, *222*, 385−386.
(3) (a) Tobe, M. L.; Burgess, J. *Inorganic Reaction Mechanisms*; Addison-Wesley Longman: Essex, England, 1999. (b) Wilkins, R. G. *Kinetics and Mechanisms of Reactions of Transition Metal Complexes*; VCH: Weinheim, Germany, 1991. (c) Tobe, M. L. In *Comprehensive Coordination Chemistry*; Wilkinson, G., Ed.; Pergamon Press: Oxford, U.K., 1987; Vol. 1, pp 311−329. (d) Atwood, J. D. *Inorganic Organometallic Reaction Mechanisms*; Brook/Cole: Monterey, CA, 1985. (e) Basolo, F.; Pearson, R. G. *Mechanisms of Inorganic Reactions*; Wiley: New York, 1968. (f) Langford, C. H.; Gray, H. B. *Ligand Substitution Processes*; W. A. Benjamin: New York, 1965. (g) Basolo, F. *Coord. Chem. Rev.* **1996**, *154*, 151−161.
(4) (a) Otto, S.; Elding, L. I. *J. Chem. Soc., Dalton Trans.* **2002**, 2354−2360. (b) Wendt, O. F.; Elding, L. I. *Inorg. Chem.* **1997**, *36*, 6028−6032. (c) Wendt, O. F.; Elding, L. I. *J. Chem. Soc., Dalton Trans.* **1997**, 4725−4731. (d) Schmülling, M.; Grove, D. M.; van Koten, G.; van Eldik, R.; Veldman, N.; Spek, A. L. *Organometallics* **1996**, *15*, 1384−1391.

 10.1021/ja030486u CCC: $27.50

of the ligands, or the discrimination ability of the substrate. New concepts have been introduced as well, such as a fine electronic tuning of the lability of Pt(II) complexes on changing systematically the nature of ancillary noninnocent ligands,[5] or making use of hyperconjugation effects, [6,7] or the possibility of inducing extra-lability[5] or fluxionality[8] to ligands through overcrowding of the coordination plane. Within this mechanistic framework, a rational control of the molecular architecture and reactivity of Pt(II) compounds is now at hand, even though the lability of these compounds will still depend in a manifold and rather intricate way on the above-mentioned factors.

A most difficult task is to induce a dissociative pathway to square-planar compounds, in view of the great electronic and steric propensity of four-coordinated 16-electron species to add a fifth ligand and to form five-coordinate 18-electron species either as discrete compounds[9] or as reaction intermediates.[3] There is a great interest in the possibility of considering alternative low-energy pathways with three-coordinate 14-electron d^8-ML_3 species as key intermediates.[10] Dissociation (usually of a neutral ligand) is often proposed as the initial step in many reactions involving square-planar d^8 organometallic complexes.[11] This dissociation enables subsequent processes such as β-hydrogen elimination,[12,13] insertion of olefins into the M−H bond,[14] reductive elimination,[15] electrophilic attack at the Pt−C bond,[16] geometrical[16,17] or configurational[18] isomerization, exchange reactions,[19] and fluxional motions of coordinated ligands.[8,20] Another promising feature of the unsaturated platinum(II) chemistry is the successful C−H activation under mild conditions by complexes of the form $[Pt(N-N)(CH_3)(solv)]^+$, where N−N is a bidentate nitrogen-centered ligand and "solv" is a weakly coordinating solvent.[21] Knowledge gained from these studies builds upon the seminal work by Shilov[22] and may allow for the catalytic activation and subsequent functionalization of one of the less reactive bonds in organic molecules.

After the first unsuccessful attempts, focused on steric blocking of the pseudo-octahedral positions[23] and/or ground-state destabilization by use of ligands with a high trans influence,[24] the first convincing evidence for the presence of three-coordinate 14-e species as key intermediates in nucleophilic substitution reactions came from kinetic studies of electron-rich complexes having a set of donor atoms of the type *cis*-[Pt(C,C)(S,S)] (C is a strong σ-donor carbon group; S = thioether or sulfoxide).[25−31] The underpinnings of the observed easy dissociation are: (i) bond weakening at the leaving group due to the trans influence of strong σ-donors, (ii) high electron density at the metal which prevents the axial approach of the incoming nucleophile, and (iii) the stabilization by the remaining set of three in-plane ligands of a three-coordinated T-shaped 14-e intermediate without changing the singlet ground state. Also, it has become evident that other appropriate sets of strong σ-donor groups can favor sufficient accumulation of electron density at the metal and stabilize the 14-e intermediate, as for *cis*-$[PtMe_2(PR_3)(dmso)]$ (PR_3 = isosteric tertiary phosphanes)[32] or *cis*-$[Pt(SiMePh_2)_2(PMe_2Ph)_2]$,[33] which shows some distortion to-

(5) Romeo, R.; Monsù Scolaro, L.; Nastasi, N.; Arena, G. *Inorg. Chem.* **1996**, *35*, 5087−5096.
(6) Romeo, R.; Plutino, M. R.; Monsù Scolaro, L.; Stoccoro, S.; Minghetti, G. *Inorg. Chem.* **2000**, *39*, 4749−4755.
(7) Hofmann, A.; Jaganyi, D.; Munro, O. Q.; Liehr, G.; van Eldik, R. *Inorg. Chem.* **2003**, *42*, 1688−1700.
(8) (a) Romeo, R.; Fenech, L.; Carnabuci, S.; Plutino, M. R.; Romeo, A. *Inorg. Chem.* **2002**, *41*, 2839−2847. (b) Romeo, R.; Fenech, L.; Monsù Scolaro, L.; Albinati, A.; Macchioni, A.; Zuccaccia, C. *Inorg. Chem.* **2001**, *40*, 3293−3302.
(9) (a) Albano, V. G.; Natile, G.; Panunzi, A. *Coord. Chem. Rev.* **1994**, *133*, 67−114. (b) Maresca, L.; Natile, G. *Comments Inorg. Chem.* **1993**, *14*, 349−366.
(10) (a) Collman, J. P.; Hegedus, L. S.; Norton, J. R.; Finke, R. C. *Principles and Applications of Organotransition Metal Chemistry*; University Science Books: Mill Valley, CA, 1987. (b) Crabtree, R. H. *The Organometallic Chemistry of the Transition Metals*; Wiley-Interscience: New York, 1994. (c) Yamamoto, A. *Organotransition Metal Chemistry*; Wiley & Sons: New York, 1986. (d) James, B. R. In *Comprehensive Organometallic Chemistry*; Wilkinson, G., Stone, F. G. A., Abel, E. W., Eds.; Pergamon Press: Oxford, 1982; Chapter 51. (e) Parshall, G. W. *Homogeneous Catalysis*; Wiley-Interscience: New York, 1980.
(11) (a) Romeo, R. *Comments Inorg. Chem.* **1990**, *11*, 21−57. (b) Puddephatt, R. J. *Angew. Chem., Int. Ed.* **2002**, *41*, 261−263. (c) Casares, J. A.; Espinet, P.; Salas, G. *Chem.-Eur. J.* **2002**, *8*, 4843−4853.
(12) For general reviews of β-elimination reactions, see: (a) Cross, R. J. In *The Chemistry of the Metal−Carbon Bond*; Hartley, F. R., Patai, S., Eds.; John Wiley: New York, 1985; Vol. 2, Chapter 8. (b) Whitesides, G. M. *Pure Appl. Chem.* **1981**, *53*, 287−292. (c) Yamamoto, A.; Yamamoto, T.; Komiya, S.; Ozawa, F. *Pure Appl. Chem.* **1984**, *56*, 1621−1634.
(13) Alibrandi, G.; Cusumano, M.; Minniti, D.; Monsù Scolaro, L.; Romeo, R. *Inorg. Chem.* **1989**, *28*, 342−347 and references therein.
(14) (a) Romeo, R.; Alibrandi, G.; Monsù Scolaro, L. *Inorg. Chem.* **1993**, *32*, 4688−4694. (b) Coussens, B. B.; Buda, F.; Oevering, H.; Meier, R. J. *Organometallics* **1998**, *17*, 795−801 and references therein.
(15) (a) Paonessa, R. S.; Trogler, W. C. *J. Am. Chem. Soc.* **1982**, *104*, 3529−3530. (b) Komiya, S.; Albright, T. A.; Hoffmann, R.; Kochi, J. K. *J. Am. Chem. Soc.* **1976**, *98*, 7255−7265. (c) Gillie, A.; Stille, J. K. *J. Am. Chem. Soc.* **1980**, *102*, 4933−4941. (d) Loar, M.; Stille, J. K. *J. Am. Chem. Soc.* **1981**, *103*, 4174−4181. (e) Moravskiy, A.; Stille, J. K. *J. Am. Chem. Soc.* **1981**, *103*, 4182−4186. (f) Ozawa, F.; Ito, T.; Nakamura, Y.; Yamamoto, A. *Bull. Chem. Soc. Jpn.* **1981**, *54*, 1868−1880.
(16) (a) Romeo, R.; Plutino, M. R.; Elding, L. I. *Inorg. Chem.* **1997**, *36*, 5909−5916. (b) Romeo, R.; Minniti, D.; Lanza, S.; Uguagliati, P.; Belluco, U. *Inorg. Chem.* **1978**, *17*, 2813−2818.
(17) (a) Romeo, R. *Comments Inorg. Chem.* **2002**, *23*, 79−100 and references therein. (b) Alibrandi, G.; Romeo, R. *Inorg. Chem.* **1997**, *36*, 6, 4822−4830. (c) Minniti, D. *Inorg. Chem.* **1994**, *33*, 2631−2634. (d) Casado, A. L.; Casares, J. A.; Espinet, P. *Inorg. Chem.* **1998**, *37*, 4154−4156.
(18) Albeniz, A. C.; Casado, A. L.; Espinet, P. *Inorg. Chem.* **1999**, *38*, 2510−2515.
(19) Scott, J. D.; Puddephatt, R. J. *Organometallics* **1983**, *2*, 1643−1648.
(20) (a) Casares, J. A.; Coco, S.; Espinet, P.; Lin, Y. S. *Organometallics* **1995**, *14*, 3058−3067. (b) Gelling, A.; Orrell, K. G.; Osborne, A. G.; Sik, V. *J. Chem. Soc., Dalton Trans.* **1998**, 937−946.
(21) (a) Stahl, S. S.; Labinger, J. A.; Bercaw, J. E. *J. Am. Chem. Soc.* **1996**, *118*, 5961−5976. (b) Labinger, J. A.; Bercaw, J. E. *Nature* **2002**, *417*, 507−514. (c) Zhong, H. A.; Labinger, J. A.; Bercaw, J. E. *J. Am. Chem. Soc.* **2002**, *124*, 1378−1399. (d) Johansson, L.; Tilset, M.; Labinger, J. A.; Bercaw, J. E. *J. Am. Chem. Soc.* **2000**, *122*, 10846−10855. (e) Procelewska, J.; Zahl, A.; van Eldik, R.; Zhong, H. A.; Labinger, J. A.; Bercaw, J. E. *Inorg. Chem.* **2002**, *41*, 2808−2810. (f) Johansson, L.; Ryan, O. B.; Tilset, M. *J. Am. Chem. Soc.* **1999**, *121*, 1974−1975. (g) Johansson, L.; Ryan, O. B.; Römming, C.; Tilset, M. *J. Am. Chem. Soc.* **2001**, *123*, 6579−6590. (h) Johansson, L.; Tilset, M. *J. Am. Chem. Soc.* **2001**, *123*, 739−740. (i) Holtcamp, M. W.; Henling, L. M.; Day, M. W.; Labinger, J. A.; Bercaw, J. E. *Inorg. Chim. Acta* **1998**, *270*, 467−478. (j) Periana, R. A.; Taube, D. J.; Gamble, S.; Taube, H.; Satoh, T.; Fujii, H. *Science* **1998**, *280*, 560−564. (k) Wick, D. D.; Goldberg, K. I. *J. Am. Chem. Soc.* **1997**, *119*, 10235−10236.
(22) (a) Gol'dshleger, N. F.; Es'kova, V. V.; Shilov, A. E.; Shteinman, A. A. *Zh. Fiz. Khim.* **1972**, *46*, 1353−1354 (English translation **1972**, *46*, 785−786). (b) Shilov, A. E.; Shul'pin, G. B. *Activation and Catalytic Reactions of Saturated Hydrocarbons in the Presence of Metal Complexes*; Kluwer Academic: Dordrecht, 2000.
(23) (a) Baddley, W. H.; Basolo, F. *J. Am. Chem. Soc.* **1966**, *88*, 2944−2950. (b) Goddard, J. B.; Basolo, F. *Inorg. Chem.* **1968**, *7*, 936−943. (c) Goddard, J. B.; Basolo, F. *Inorg. Chem.* **1968**, *7*, 2456−2458.
(24) (a) Faraone, G.; Ricevuto, V.; Romeo, R.; Trozzi, M. *Inorg. Chem.* **1969**, *8*, 2207−2211. (b) Faraone, G.; Ricevuto, V.; Romeo, R.; Trozzi, M. *Inorg. Chem.* **1970**, *9*, 1525−1528.
(25) Plutino, M. R.; Monsù Scolaro, L.; Romeo, R.; Grassi, A. *Inorg. Chem.* **2000**, *39*, 2712−2720.
(26) Frey, U.; Helm, L.; Merbach, A. E.; Romeo, R. *J. Am. Chem. Soc.* **1989**, *111*, 8161−8165.
(27) Alibrandi, G.; Minniti, D.; Monsù Scolaro, L.; Romeo, R. *Inorg. Chem.* **1989**, *28*, 1939−1943.
(28) Alibrandi, G.; Bruno, G.; Lanza, S.; Minniti, D.; Romeo, R.; Tobe, M. L. *Inorg. Chem.* **1987**, *26*, 185−190.
(29) Minniti, D.; Alibrandi, G.; Tobe, M. L.; Romeo, R. *Inorg. Chem.* **1987**, *26*, 3956−3958.
(30) (a) Lanza, S.; Minniti, D.; Moore, P.; Sachinidis, J.; Romeo, R.; Tobe, M. L. *Inorg. Chem.* **1984**, *23*, 4428−4833. (b) Lanza, S.; Minniti, D.; Romeo, R.; Moore, P.; Sachinidis, J.; Tobe, M. L. *J. Chem. Soc., Chem. Commun.* **1984**, 542−543.
(31) Minniti, D. *J. Chem. Soc., Dalton Trans.* **1993**, 1343−1345.
(32) Romeo, R.; Monsù Scolaro, L.; Plutino, M. R.; Bottari, G.; Romeo, A. *Inorg. Chim. Acta* **2003**, *350*, 143−151.
(33) Wendt, O. F.; Deeth, R. J.; Elding, L. I. *Inorg. Chem.* **2000**, *39*, 5271−5276.

Scheme 1

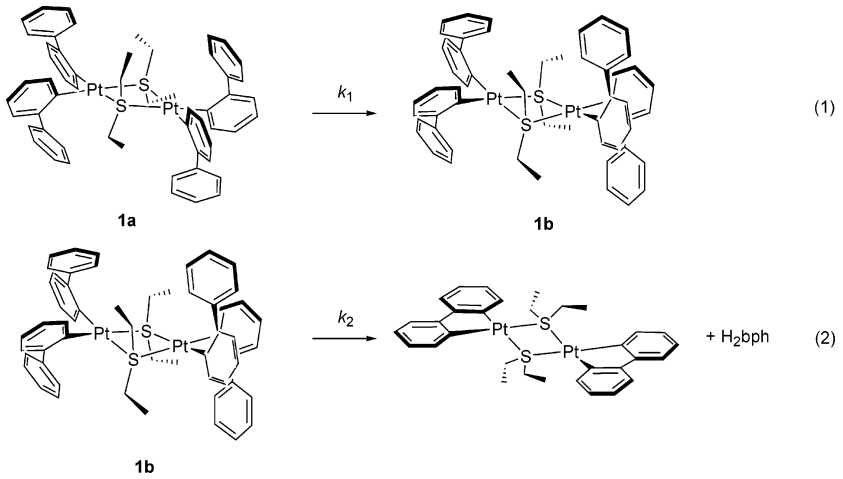

ward a tetrahedral arrangement. These favorable factors do not apply to ligands which exhibit major π-acceptor capabilities, as for *cis*-[$PtPh_2(CO)(SMe_2)$], where the relief of the excess of electron density at the metal by carbon monoxide and the presence of a low-lying LUMO, π-delocalized over the Pt−C−O atoms, facilitate a changeover of mechanism from dissociative to associative.[34] The 2,2′-biphenyl dianion (bph^{2-}), a cyclometalating analogue of 2,2′-bipyridine, combines cyclometalation and a favorable in-plane disposition of the aryl rings for π interaction: contrary to expectation, recent kinetic and theoretical studies of the complexes [$Pt(bph)(SR_2)_2$][25] indicated that thioether dissociation is much easier than in the diaryl analogue *cis*-[$PtPh_2(SR_2)_2$]. Back-donation from filled d orbitals of the metal to empty π^* orbitals of the in-plane cyclometalated rings is weak or absent and is not operative in promoting an associative mode of activation.

We report here a detailed kinetic study of ligand (dmso) exchange and substitution (by 2,2′-bipyridine and 1,10-phenanthroline) on the complex *cis*-[$Pt(Hbph)_2(dmso)_2$] ($Hbph^- = \eta^1$-biphenyl monoanion). The results are consistent with a dissociative mode of activation by analogy with the behavior already found for similar [Pt(C,C)(S,S)] compounds. The kinetic data on these systems are now adequate to establish to what extent dissociation depends on the nature of the bonded organic moiety (alkyl or aryl), its size, and its orientation with respect to the coordination plane. During the synthetic workup, we observed the formation of a new dinuclear platinum(II) compound with thioether bridges of formula [$Pt_2(\mu\text{-}SEt_2)_2(Hbph)_4$], **1a**, which in chloroform undergoes atropisomerization to **1b** followed by C−H activation to yield [$Pt_2(bph)_2(\mu\text{-}SEt_2)_2$] (bph = 2,2′-biphenyl dianion) and biphenyl. The conformations of **1a** and **1b** were characterized by NMR spectroscopy and molecular mechanics calculations, and the interconversion and cyclometalation were monitored by ^{1}H NMR.

Results

Synthesis and Structure of Complexes. In the dinuclear complex **1a**, obtained in a pure form from the reaction of 2,2′-dilithiumbiphenyl (in a 2:1 stoichiometric ratio) with *cis*-[$Pt(SEt_2)_2Cl_2$] in Et_2O (19% yield), each metal atom is in a square-planar environment and the biphenyl monoanion is η^1-coordinated to the metal. The complex is slightly soluble in chlorinated solvents where it undergoes a slow conversion to the species **1b**, as depicted in eq 1 of Scheme 1. Finally, intramolecular C−H activation on the isomer **1b** affords the dinuclear cyclometalated species [$Pt_2(\mu\text{-}SEt_2)_2(bph)_2$], the only product isolated and characterized originally by von Zelewsky et al.[35] using the same procedure (eq 2, Scheme 1).

Compound **1a** is a useful synthon for the synthesis of mononuclear platinum(II) derivatives containing the organometallic skeleton Pt(C,C) in a head-to-tail conformation: (i) addition of 2 equiv of dimethyl sulfoxide or diethyl sulfide per platinum(II) yielded complexes **3** and **4**, respectively; (ii) bridge splitting reactions with bidentate nitrogen ligands (bpy or phen) afforded the diimine-containing species **5** and **6**, respectively. All of the experimental evidence, including the X-ray molecular structure of **5** and **6** (see below), showed the two Hbph fragments to be tilted from the coordination plane and in a head-to-tail conformation. These species maintain an apparently stereochemically rigid structure in solution (unchanged ^{1}H and ^{13}C NMR spectra up to 333 K) because of restricted rotation of the $Hbph^-$ ligands around the Pt−C bond.[36]

A view of the structures of compounds **5** and **6**, the first reported so far for platinum(II) compounds with η^1-$Hbph^-$ ligands, is given in Figures 1 and 2. Crystallographic data and selected bond distances and angles are listed in Tables 1 and 2, respectively. Both complexes possess a slightly distorted square-planar coordination consisting of the two nitrogen atoms of the bipy and phen ligands, respectively, and one carbon atom from each of the two biphenyl moieties. The Pt−C and Pt−N distances were found to be substantially identical (within 3σ's) in both compounds [av. 2.00(3) and 2.10(2) Å, respectively]. The Pt−C distances are as expected[37] and can be compared to

(34) Romeo, R.; Grassi, A.; Monsù Scolaro, L. *Inorg. Chem.* **1992**, *31*, 4383−4390.

(35) Cornioley-Deuschel, C.; von Zelewsky, A. *Inorg. Chem.* **1987**, *26*, 3354−3358.

(36) Some other selected examples of restricted aryl rotation around the M−C bond are as follows: (a) Brown, J. M.; Pérez-Torrente, J. J.; Alcock, N. W. *Organometallics* **1995**, *14*, 1195−1203. (b) Rieger, A. L.; Carpenter, G. B.; Rieger, P. H. *Organometallics* **1993**, *12*, 842−847. (c) Anderson, G. K.; Cross, R. J.; Manojlovíc-Muir, L.; Muir, K. W. *Organometallics* **1988**, *7*, 1520−1525. (d) Albeniz, A. C.; Casado, A. L.; Espinet, P. *Organometallics* **1997**, *16*, 5416−5423. (e) Casares, J. A.; Coco, S.; Espinet, P.; Lin, Y. S. *Organometallics* **1995**, *14*, 3058−3067. (f) Albeniz, A. C.; Casado, A. L.; Espinet, P. *Inorg. Chem.* **1999**, *38*, 2510−2515. (g) Anderson, G. K.; Black, D. M.; Cross, R. J.; Robertson, F. J.; Rycroft, D. S.; Wat, R. K. M. *Organometallics* **1990**, *9*, 2568−2574.

(37) *International Tables for X-ray Crystallography*, 2nd ed.; Kluwer Academic: Dordrecht, NL, 1999; Vol. C, Chapters 9.5 and 9.6.

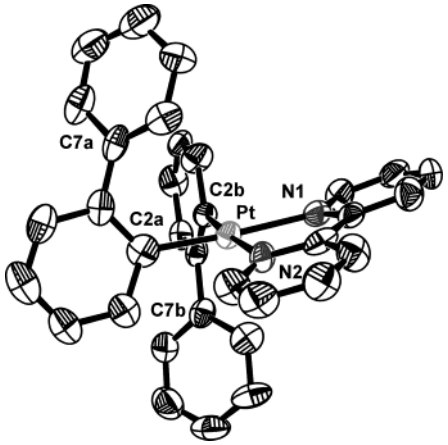

Figure 1. ORTEP view of a molecule of compound **5** showing 50% probability ellipsoids for the non-hydrogen atoms.

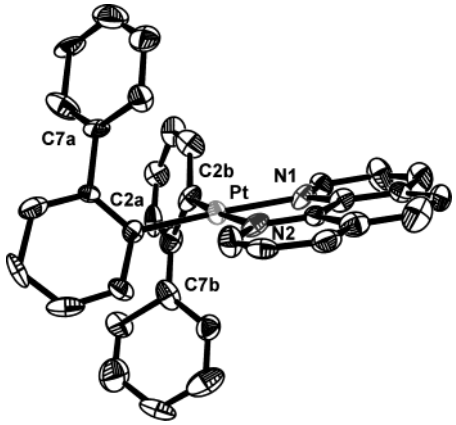

Figure 2. ORTEP view of a molecule of compound **6** showing 50% probability ellipsoids for the non-hydrogen atoms.

those found in similar complexes, for example, in [Pt(mesityl)$_2$-(dppz)] [av. 2.00(1) Å],[38] in [Pt (2,9-dmphen)R$_2$] (R = Ph, mesityl), and in [Pt(mesityl)$_2$(phen)] [av. 2.016(5) Å].[39] A similar trend can be found for the Pt−N distances: values around 2.10 Å are found in the above-mentioned complexes and in the literature.[40] As expected, the angles at the Pt atom are constrained by the bite of the chelating ligand. Thus, for compound **5**, the N1−Pt−N2 angle is 77.6(4)°, while for **6** it is 79.0(2)°. Moreover, the angles with the trans ligand (i.e.: N1−Pt−C2a and N2−Pt−C2b), of ca. 175° and 173°, are close to their ideal values. In both complexes, a small tetrahedral distortion is observed, with maximum deviations of the atoms coordinated to the platinum center from their lsq-plane of ca. ±0.03 Å for **6** and ±0.06 Å for **5**. The bpy and phen ligands also lie in the coordination plane; the dihedral angle between the lsq-plane defined by atoms Pt, C2a, C2b and that defined by the C atoms of the bipyridine is 9.7(5)°, while the corresponding angle in **6** is 1.3(1)° only. It may also be noted that the two rings of the bpy ligand are not coplanar, but are rotated by 5.9(7)°, as a consequence of the coordination to the metal.

The rings of the biphenyl moieties are tilted with respect to the coordination plane, as judged from: (i) the relevant torsion angles in Table 2, and (ii) the dihedral angles between the lsq-planes C1a−C6a and C1b−C6b and that defined by Pt−N1−N2. Thus, in **5**, these angles are 76.4(3)° and 78.9(3)°, respectively, while in **6** the corresponding values are 71.2(5)° and 62.4(3)°. The biphenyl moieties are in both compounds in a head-to-tail disposition (see Figures 1 and 2). Moreover, the two rings are not coplanar, but rotated by 43.7(5)° and 46.8(5)°, respectively, in **5**; for **6**, the corresponding values are 52.4(5)° and 62.4(3)°. There is no significant inter- or intramolecular stacking ($\pi-\pi$ interactions). The shortest intermolecular separations are found in **6** between the phenyl rings and the phenanthroline ligand of symmetry related molecules (in the range 4.8−5.1 Å).

Table 1. Experimental Data for the X-ray Diffraction Study of Compounds [Pt(Hbph)$_2$(bpy)] (**5**) and [Pt(Hbph)$_2$(phen)]·(C$_7$H$_8$) [**6**·(C$_7$H$_8$)]

compound	**5**	**6**·(C$_7$H$_8$)
formula	$C_{34}H_{24}N_2Pt$	$C_{43}H_{26}N_2Pt$
mol wt	655.64	765.75
diffractometer	CAD4	Bruker SMART CCD
cryst syst	monoclinic	monoclinic
space group	$P2_1/n$	Cc
T, K	298 (2)	200 (2)
a, Å	14.006 (4)	17.5109 (3)
b, Å	12.901 (3)	11.4963 (2)
c, Å	14.637 (6)	17.9161 (2)
β, deg	107.13 (4)	115.058 (1)
V, Å^3	2527 (2)	3267.2 (1)
Z	4	4
$\rho_{(calcd)}$, g cm^{-3}	1.723	1.557
μ, cm^{-1}	55.78	43.28
radiation	Mo Kα (graphite monochromated λ = 0.71069 Å)	
θ range (deg)	$3.0 < \theta < 23.0$	$2.2 < \theta < 27.5$
no. data coll	3643	16 265
no. independent data	3487	7312
no. obs reflns (n_o)	2076 $[\lvert F_o\rvert^2 > 4.0\sigma(\lvert F\rvert^2)]$	6072 $[\lvert F_o\rvert^2 > 4.0\sigma(\lvert F\rvert^2)]$
transmission coeff	0.86−1.00	0.60−0.98
R_{av}[a]	0.050	0.040
R[b] (obs reflns)	0.0398	0.0352
R_w^2 [c]	0.0962	0.0757
GOF[d]	0.982	0.976

[a] $R_{av} = \sum\lvert F_o^2 - F_{o,av}^2\rvert/\sum_i\lvert F_o^2\rvert$. [b] $R = \sum(\lvert F_o - (1/k)F_c\rvert)/\sum\lvert F_o\rvert$. [c] $R_w^2 = [\sum w(F_o^2 - (1/k)F_c^2)^2/\sum w\lvert F_o^2\rvert^2]$. [d] GOF: $[\sum_w(F_o^2 - (1/k)F_c^2)^2/(n_o - n_v)]^{1/2}$.

Table 2. Selected Bond Lengths (Å), Bond Angles (deg), and Dihedral Angles (deg) for [Pt(Hbph)$_2$(bpy)] (**5**) and [Pt(Hbph)$_2$(phen)] (**6**)

	[Pt(Hbph)$_2$(bpy)] (**5**)	[Pt(Hbph)$_2$(phen)] (**6**)
Pt−N(1)	2.11(1)	2.10(1)
Pt−N(2)	2.08(1)	2.11(1)
Pt−C(2a)	2.01(1)	1.97(2)
Pt−C(2b)	1.99(1)	2.03(2)
N(1)−Pt−N(2)	77.6(4)	79.0(2)
N(1)−Pt−C(2b)	97.5(4)	96.6(5)
N(2)−Pt−C(2a)	96.5(4)	95.3(6)
C(2a)−Pt−C(2b)	88.4(5)	89.1(2)
N(1)−Pt−C(2b)−C(3b)	−78.8(9)	−69(1)
N(2)−Pt−C(2a)−C(3a)	−75(1)	−71(1)
C(2a)−C(1a)−C(7a)−C(8a)	−47(2)	−53(2)
C(2b)−C(1b)−C(7b)−C(8b)	−48(2)	−51(2)

NMR Conformational Analysis. All of the proton and carbon resonances belonging to the species **1**−**6** were assigned through NMR spectroscopy from the connectivities in 2D-COSY and ^{13}C,^{1}H-HMQC experiments. Sketches of complexes **1**−**6**, together with the adopted numbering scheme, are given in Chart 1. The relevant ^{1}H and ^{13}C NMR data are collected in Tables 3 and 4, respectively. ^{1}H NMR spectra on freshly dissolved

(38) Klein, A.; Scheiring, T.; Kaim, W. *Z. Anorg. Allg. Chem.* **1999**, *625*, 1177−1180.
(39) Klein, A.; McInnes, E. J. L.; Kaim, W. *J. Chem. Soc., Dalton Trans.* **2002**, 2371−2378.
(40) Allen, F. H. *Acta Crystallogr*. **2002**, *B58*, 380−388.

Table 3. Collection of the ^{1}H NMR Resonances of the Platinum(II) Complexes **1**−**6**[a]

	δ^1H (J_{PtH})							
	$H_{3a,3b}$ ($^3J_{PtH}$)	$H_{4a,4b}$ ($^4J_{PtH}$)	$H_{5a,5b}$	$H_{6a,6b}$ ($^4J_{PtH}$)	$H_{8a,12a}$+$H_{8b,12b}$	$H_{9a,11a}$+$H_{9b,11b}$	$H_{10a,10b}$	others
1a	6.28 (71.0)	6.52	6.71	6.84	7.61	7.41	7.41	2.69 (S−CH_{2b}−CH_3), 2.67 (S−CH_{2a}−CH_3), 2.00 (S−CH_2−CH_{3a}), 0.29 (S−CH_2−CH_{3b})
1b	6.48 (69.0)	6.64	6.81	6.94	7.58	7.43	7.33	3.40 (S−CH_{2a}−CH_3), 3.19 (S−CH_{2b}−CH_3), 2.94 (S−C$H_{2a'}$−CH_3), 2.88 (S−C$H_{2b'}$−CH_3), 1.83 (S−CH_2−CH_{3a}), 1.30 (S−CH_2−CH_{3b})
2	6.20 (69.3)	6.64 (13.8)	6.76	6.93 (26.4)	7.44	7.33	7.33	5.05 ($^2J_{PtH}$ = 42.8 Hz, $CH_{1,5}$), 4.81 ($^2J_{PtH}$ = 39.2 Hz, $CH_{2,6}$), 2.46+2.36 ($(CH_2)_{4,8}$), 2.30 ($(CH_2)_{3,7}$)
3	5.85 (73.4)	6.57 (13.5)	6.82	7.06 (20.3)	7.85	7.39	7.36	3.10 ($^3J_{PtH}$ = 12.1, S−CH_{3a}), 2.29 ($^3J_{PtH}$ = 16.0, S−CH_{3b})
4	6.59 (78.8)	6.59	6.76	7.03 (23.4)	7.96	7.30	7.26	2.31 ($^3J_{PtH}$ = 25.8, S−CH_2−CH_3), 1.13 (S−CH_2−CH_3)
5	6.79 (70.5)	6.71	6.87	7.12	7.77	7.05	7.05	8.41 ($^3J_{PtH}$ = 22.6 Hz, $H_{6,6'}$), 7.97 ($H_{4,4'}$), 7.89 ($H_{3,3'}$), 7.25 ($H_{5,5'}$)
6	6.90 (71.8)	6.77	6.93	7.17	7.82	6.98	6.98	8.68 ($^3J_{PtH}$ = 21.1, $H_{2,9}$), 8.45 ($H_{4,7}$), 7.86 ($H_{5,6}$), 7.57 ($H_{3,8}$)

[a] Recorded in $CDCl_3$ as solvent at 298.2 K. Chemical shifts (δ) in ppm relative to TMS and coupling constants, given in parentheses together with the assignment, in hertz.

Table 4. Collection of the ^{13}C{^{1}H} NMR Resonances of the Platinum(II) Complexes **1**−**6**[a]

	δ^{13}C (J_{PtC})										
	$C_{1a,1b}$ ($^2J_{PtC}$)	$C_{2a,2b}$ ($^1J_{PtC}$)	$C_{3a,3b}$ ($^2J_{PtC}$)	$C_{4a,4b}$ ($^3J_{PtC}$)	$C_{5a,5b}$ ($^4J_{PtC}$)	$C_{6a,6b}$ ($^3J_{PtC}$)	$C_{7a,7b}$ ($^3J_{PtC}$)	$C_{8a,12a}$+ $C_{8b,12b}$	$C_{9a,11a}$+ $C_{9b,11b}$	$C_{10a,10b}$	others
1a[b]	−[c]	−[c]	135.7	125.2	122.2	128.8	−[c]	129.7	127.2	125.8	33.1 (S−CH_{2b}−CH_3), 22.8 (S−CH_{2a}−CH_3), 11.9 (S−CH_2−CH_{3a}), 9.51 (S−CH_2−CH_{3b})
1b	−[c]	−[c]	136.1	125.3	122.5	129.2	−[c]	127.2	128.8	127.0	33.7 (S−CH_{2b}−CH_3), 33.3 (S−C$H_{2b'}$−CH_3), 30.5 (S−CH_{2a}−CH_3), 30.3 (S−C$H_{2a'}$−CH_3), 12.9 (S−CH_2−CH_{3a}), 12.5 (S−CH_2−CH_{3b})
2	148.0 (39)	151.4 (1117)	136.2 (14)	125.7 (68)	122.4 (9)	129.0 (59)	146.6 (34)	129.7	127.1	125.9	108.2 ($^1J_{PtC}$ = 67 Hz, $C_{1,5}$), 99.7 ($^1J_{PtC}$ = 41 Hz, $C_{2,6}$), 30.9 ($C_{4,8}$), 28.4 ($C_{3,7}$)
3	147.1 (41)	143.5 (1041)	136.4 (26)	125.8 (73)	123.6 (11)	128.9 (57)	146.5 (28)	129.8	127.3	126.2	43.9 ($^2J_{PtC}$ = 20 Hz, S−CH_{3a}), 42.3 ($^2J_{PtC}$ = 37 Hz, S−CH_{3b})
4	148.3 (42)	146.5 (1137)	138.1 (22)	125.1 (79)	121.7 (10)	128.4 (62)	146.2 (25)	130.0	126.8	125.3	27.6 (S−CH_2−CH_3), 13.1 ($^3J_{PtC}$ = 16 Hz, S−CH_2−CH_3)
5	148.6	144.3	140.2	125.1	121.9	128.0	147.9	130.1	126.4	124.6	155.7 ($C_{2,2'}$), 150.1 ($C_{6,6'}$), 135.7 ($C_{4,4'}$), 129.9 ($C_{3,3'}$), 126.9 ($C_{5,5'}$)
6	148.6	144.3	140.1	125.1	121.5	128.0	147.9	130.1	126.3	124.6	155.6 ($C_{10,10'}$), 151.3 ($C_{4',6'}$), 150.1 ($C_{2,9}$), 135.7 ($C_{4,7}$), 126.9 ($C_{5,6}$), 125.4 ($C_{3,8}$)

[a] Recorded in $CDCl_3$ as solvent at 298.2 K. Chemical shifts (δ) in ppm relative to TMS and coupling constants, given in parentheses together with the assignment, are in hertz. [b] At T = 273 K. [c] Not detectable.

samples of **1a** in $CDCl_3$ reveal a pattern of signals typical of a pair of η^1-biphenyl ligands spanning mutual cis positions, with resonances at δ 7.61 ($H_{8a,12a}$+$H_{8b,12b}$), 7.41 ($H_{9a,11a}$+$H_{9b,11b}$+$H_{10a,10b}$), 6.84 ($H_{6a,6b}$), 6.71 ($H_{5a,5b}$), 6.52 ($H_{4a,4b}$), and 6.28 ($^3J_{PtH}$ = 71.0 Hz, $H_{3a,3b}$). The *ortho*-protons $H_{3a,3b}$ were unambiguously attributed on the basis of the satellite peaks due to coupling with ^{195}Pt nuclei (I = $^1/_2$, 33% natural abundance). The pattern of the aromatic region in this compound is symmetric and strictly similar to that observed for the mononuclear complexes **3**−**6** containing the same molecular fragment *cis*-[Pt(Hbph)$_2$] in a head-to-tail conformation. In fact, these mononuclear species are formed upon bridge-splitting reaction of various ligands on **1a** (see Experimental Section) and retain memory of the *cis*-[Pt(Hbph)$_2$] conformation of the dinuclear precursor. The aliphatic region shows a composite multiplet at δ 2.69 (4H, S−CH_{2b}−CH_3) and 2.67 (4H, S−CH_{2a}−CH_3), and two well-separated triplets relative to the methyl protons at δ 2.00 (6H, S−CH_2−CH_{3a}) and 0.29 (6H, S−CH_2−CH_{3b}). By lowering the temperature to 223 K, the multiplet relative to the methylene protons of the bridging diethyl sulfide separates into a pair of well-resolved broad quartets at 2.75 and 2.65 ppm, together with the two expected triplets at 2.09 and 0.27 ppm for the methyl groups. Interestingly, the structure of strictly similar compounds,

Chart 1. Sketches for Complexes **1**−**6**, Together with the Adopted Numbering Scheme

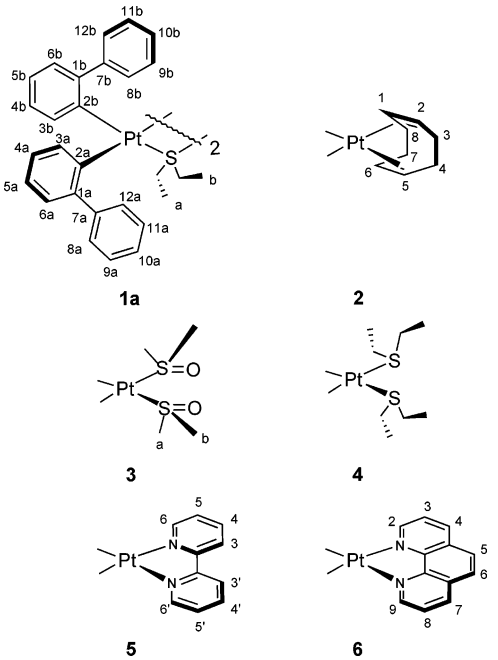

Chart 2. Lowest Energy Calculated Structures of the $\alpha\beta\beta\alpha$ (**1a**) and $\alpha\beta\alpha\beta$ (**1b**) Conformations of $[Pt_2(Hbph)_4(\mu\text{-}SEt_2)_2]$ Together with the Schematic Representations of the Five Possible Atropisomers and Relative Differences in Strain Energies (kcal/mol)

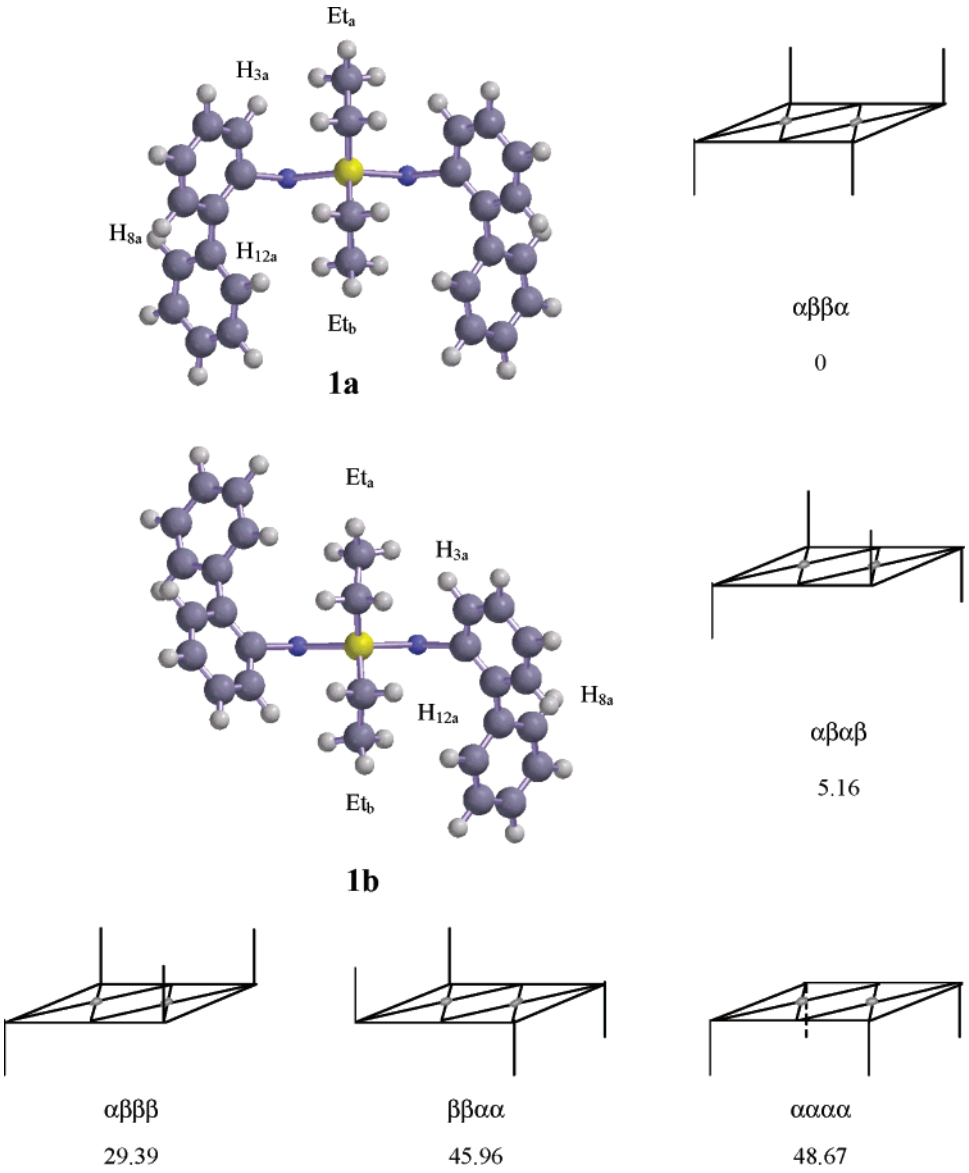

$[Pt_2Me_4(\mu\text{-}SEt_2)_2]$[41] and $[Pt_2(p\text{-tol})_4(\mu\text{-}SEt_2)_2]$,[42] consists of centrosymmetric dimers with a planar Pt_2S_2 unit. In the latter compound, the C_6 plane of the *p*-tolyl groups forms angles of 78.85° [C(1−6)] and 65.56° [C(8−13)] with the Pt_2S_2 plane. The diethyl sulfide ligands are symmetrically coordinated to Pt(1) and Pt(2), and no significant bonding interaction between the platinum atoms was found.[43]

On standing at 298 K, **1a** progressively converts into the cyclometalated species $[Pt_2(bph)_2(\mu\text{-}SEt_2)_2]$ and biphenyl, according to eq 2 in Scheme 1. ^{1}H NMR spectra showed the intermediacy of **1b** in this process, with a pattern closely similar to that of the parent **1a**, which implies the presence of the molecular fragments *cis*-$[Pt(Hbph)_2]$, together with bridging diethylthioethers.

Because of the different relative orientations of the four surrounding η^1-biphenyl anions, a series of at least five rotational isomers or atropisomers can be predicted for **1a**. Molecular mechanics force field (MMFF) minimized molecular models of such species, together with the calculated differential values of their potential energy, are shown in Chart 2. As expected,

(41) Bancroft, D. P.; Cotton, F. A.; Falvello, L. R.; Schwotzr, W. *Inorg. Chem.* **1986**, *25*, 763−770.
(42) Casado Lacabra, M. A.; Canty, A. J.; Lutz, M.; Patel, J.; Spek, A. L.; Sun, H.; van Koten, G. *Inorg. Chim. Acta* **2002**, *327*, 15−19.

(43) In view of the recent observation of a cyclic trimeric structure for $[PtPh_2(SMe_2)]_3$ (Song, D.; Wang, S. *J. Organomet. Chem.* **2002**, *648*, 302−305), in addition to the well-known dinuclear structures of $[Pt_2Ph_4(\mu\text{-}SMe_2)_2]$ and of similar thioether-bridged platinum(II) compounds (see refs 41 and 42), a referee has suggested an additional control of the structure adopted by the diaryl compound **1a**. Fast atom bombardment mass spectrometry (FABMS) analysis of **1a**, with a Xenon pressure of 10^{-5} Torr, 6 keV energy, and 1 mA ion current, gave extensive and indeterminate fragmentation. In the matrix-assisted laser-desorption-ionization mass spectrometry analysis (MALDI-TOF-MS; matrix: 2,5-dihydroxybenzoic acid in CH_2Cl_2), the highest *m*/*z* ion observed, at 1001.20, corresponds to the protonated fragment $[M - R_1 - R_2 + H]^+$ arising from the loss of a bis-phenyl ($R_1 = C_{12}H_9$) and an ethyl ($R_2 = C_2H_5$) group from **1a**. Both the position of the highest *m*/*z* peak in the MALDI-TOF spectrum and the isotope distribution, which is very close to the calculated one (see Figure S3 in the Supporting Information), provide unambiguous evidence for a dimeric structure. Monomeric or trimeric Pt(II) species should exhibit markedly different isotopic distributions. The spontaneous isomeric conversion of **1a** into **1b** in dichloromethane was monitored for 5 h at room temperature by ^{1}H NMR, after which the sample showed a MALDI-TOF peak pattern coincident with that obtained for **1a**, together with other fragments due to the final cyclometalated dinuclear product, thus confirming that the conversion of **1a** onto **1b** is indeed an isomerization process.

different atropisomers exhibit different stability and in particular those having at least a head-to-head disposition of the Hbph groups on a metal atom ($\alpha\beta\beta\beta$, $\beta\beta\alpha\alpha$, and $\alpha\alpha\alpha\alpha$). The most stable conformations are the alternating $\alpha\beta\beta\alpha$ and $\alpha\beta\alpha\beta$, characterized by a head-to-tail arrangement of the Hbph groups on both metal centers. Chart 2 reports also side views of the two atropisomers **1a** and **1b**, which clearly display largely different chemical environments for the two ethyl groups on the sulfur atom of a bridging thioether. The experimental observation of symmetrical patterns for the aromatic region of **1a** and **1b** rules out the higher energy atropisomers, and the NMR evidence, together with 2D-NOE experiments (Table S13 reports a complete map of the observed nOe dipolar contacts), points to the alternating species $\alpha\beta\beta\alpha$ and $\alpha\beta\alpha\beta$.

Now, we must address the problem of establishing the relative conformations of **1a** and **1b**. The mutual cis position and the predominance of a head-to-tail disposition of the two pendant aryl groups in the *cis*-[Pt(Hbph)$_2$] fragment of **1a** are fully confirmed by strong interligand nOe's cross-peaks between the $H_{8a,12a}$ protons of a Ph−C fragment and the H_{3b} proton that lies in front of them, on the opposite cis phenyl ring directly coordinated to platinum(II). Furthermore, the resonances of the *ortho*-protons $H_{3a,3b}$ ($\delta = 6.28$ ppm) are consistently shifted to lower frequencies with respect to those of the similar $H_{2,6}$ protons in complexes of the type *cis*-[Pt(Ph)$_2$(SR$_2$)][27] (R = a series of alkyl and aryl groups, $\delta = 7.2-7.7$ ppm) or in *cis*-[Pt(Ph)$_2$(dmso)$_2$][30] ($\delta = 7.26$ ppm), as a result of ring current from the phenyl substituent [C(7−12)] on the Hbph group bound in the cis position to the same metal center. Intense cross-peaks are also evident between $H_{8a,12a}$ and $H_{9a,11a}$ on Hbph substituents belonging to different metal centers. Particularly diagnostic in establishing the conformation of **1a** were the intramolecular cross-peaks between aliphatic (SEt$_2$) and aromatic Hbph protons. The methylene protons (S−CH_2−CH$_3$) of the central diethyl sulfide show two nOe contacts, at δ 2.69+2.67 ppm, with $H_{8a,12a}$ and H_{3a}. Most important, while the triplet of the methyl protons (S−CH$_2$−CH_{3a}) at 2.00 ppm evidences a major nOe cross-peak with H_{3a}, the signal at 0.29 ppm (S−CH$_2$−CH_{3b}) has only a selective nOe contact with $H_{8a,12a}$. The relevant difference of chemical shift between the two methyl groups is indicative of a large diversity in the magnetic environments for these groups on the same sulfur atom, and therefore the $\alpha\beta\beta\alpha$ conformation remains the most probable one for **1a**.

Phase-sensitive ^{1}H NOESY experiments on a chloroform-*d* solution of **1a**, cooled at 273 K after 12 h of standing at ambient temperature, showed the presence of both **1a** and **1b**, together with the final cyclometalated species [Pt$_2$(bph)$_2$(μ-SEt$_2$)$_2$] and free biphenyl (Figure 3). As expected for an $\alpha\beta\alpha\beta$ conformation, each methylene group of a bridging SEt$_2$ ligand in **1b** is diastereotopic, as evidenced by the two pairs of multiplets (see Table 3). The separation between the methyl peaks (triplets, S−CH$_2$−CH_{3a}, 1.83 ppm; S−CH$_2$−CH_{3b}, 1.30 ppm) is smaller than in **1a**. Additional evidence for the $\alpha\beta\alpha\beta$ conformation in **1b** comes from other specific nOe contacts between the aromatic and the aliphatic proton signals listed in Table S13 of the Supporting Information.

The methylene resonances of all three Pt(II) compounds (**1a**, **1b**, and [Pt$_2$(bph)$_2$(μ-SEt$_2$)$_2$]) show the expected nOe cross-peaks with the corresponding methyl protons, and in **1b** there are nOe contacts between the couples of diastereotopic protons. From

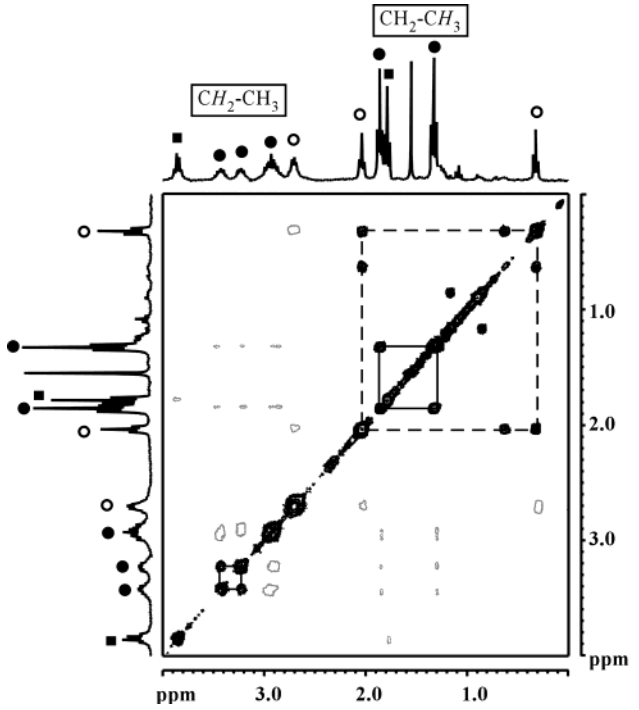

Figure 3. Aliphatic section of the phase-sensitive ^{1}H-2D NOESY spectrum relative to a chloroform-*d* solution of the two atropisomers **1a** (empty circles) and **1b** (filled circles), and the cyclometalated species [Pt(bph)(SEt$_2$)]$_2$ (filled squares) at 273 K. The "filled-in" cross-peaks arise from exchange, whereas the "open" cross-peaks arise from nOe's.

the ^{1}H NOESY experiment in Figure 3, it is possible to infer the occurrence of chemical exchange on the NMR time-scale between the ethyl groups belonging to the same sulfur atom. Well-resolved exchange cross-peaks are evident for the eight protons of the four methylene signals in **1b** and for the 12 protons of the two magnetically unequivalent methyl protons in each isomer. The most probable mechanism for this dynamic process involves preliminary bridge splitting and subsequent inversion of configuration at the uncoordinated sulfur atom. This latter process is well known for chalcogen donor atoms (S, Se, and Te) in metal complexes,[44] usually determining interchange of diastereotopic protons belonging to prochiral methylene groups, and for dinuclear species containing the Pt_2S_2 unit.[45] Furthermore, a series of additional intense cross-peaks suggests the presence of minor fast exchanging species, which could contribute to the overall process.

Kinetics: (i) Atropisomerization and Cyclometalation. Freshly prepared chloroform solutions of the dinuclear species **1a** ($\alpha\beta\beta\alpha$) evolve irreversibly toward the cyclometalated species [Pt$_2$(bph)$_2$(μ-SEt$_2$)$_2$] and free biphenyl, through the intermediacy of the unstable conformer **1b** ($\alpha\beta\alpha\beta$). The overall reaction is described as a sequence of two irreversible consecutive steps (eqs 1 and 2 in Scheme 1). The NMR features of the final cyclometalated product were reported previously.[35] The integrals of selected peaks of all species were measured as a function of time, and the relative calculated concentrations were used in the fitting procedure (Figure 4). The rate of the first step, the

(44) (a) Abel, E. W.; Bhargava, S. K.; Orrell, K. G. *Prog. Inorg. Chem.* **1984**, *32*, 1−118. (b) Gummin, D. D.; Ratilla, E. M. A.; Kostic, N. M. *Inorg. Chem.* **1986**, *25*, 2429−2433. (c) Galbraith, J. A.; Menzel, K. A.; Ratilla, E. M. A.; Kostic, N. M. *Inorg. Chem.* **1987**, *26*, 2073−2078.
(45) Abel, E. W.; Evans, D. G.; Koe, J. R.; Hursthouse, M. B.; Maxid, M.; Mahon, M. F.; Molloy, K. C. *J. Chem. Soc., Dalton Trans.* **1990**, 1697−1704.

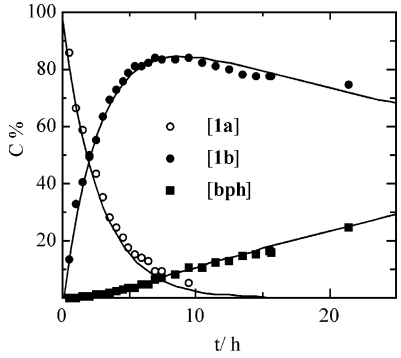

Figure 4. Time dependence of the concentration of starting dinuclear complex **1a**, the intermediate **1b**, and the final biphenyl cyclometalated species for the cyclometalation reaction as described in Scheme 1 [$k_1 = (1.03 \pm 0.01) \times 10^{-4}$ s^{-1}; $k_2 = (4.48 \pm 0.05) \times 10^{-6}$ s^{-1}, in chloroform at 298 K].

atropisomerization process, was measured by following the disappearance with time of the methylene signals relative to the coordinated diethyl sulfide in **1a** (at δ 2.69−2.67). The value of the rate constant $k_1 = (1.03 \pm 0.01) \times 10^{-4}$ s^{-1} was calculated by a nonlinear least-squares fit to the equation

$$[\mathbf{1a}]_t = [\mathbf{1a}]_0 \exp(-k_1 t) \quad (3)$$

where $[\mathbf{1a}]_0$ is the concentration of the starting complex at the beginning of the reaction. The rate of the second step (cyclometalation) was obtained by monitoring the diethyl sulfide methylene resonances of both the intermediate species **1b** (four peaks in the 3.40−2.88 ppm range) and the final cyclometalated complex $[Pt_2(bph)_2(\mu\text{-}SEt_2)_2]$ (**bph**) (at δ 3.82). The values of the concentrations derived from the integrals were fitted to the equations:

$$[\mathbf{1b}]_t = [\mathbf{1a}]_0[k_1/(k_2 - k_1)][\exp(-k_1 t) - \exp(-k_2 t)] \quad (4)$$

$$[\mathbf{bph}]_t = [\mathbf{1a}]_0 - [\mathbf{1a}]_t - [\mathbf{1b}]_t \quad (5)$$

which describe the time dependence of [**1b**] and [**bph**], respectively. The values of k_1 and k_2 derived from a global best fitting analysis using eqs 3−5 and the SCIENTIST program[46] were in good agreement with the values obtained from the separate application of eqs 3 and 4.

(ii) Dimethyl Sulfoxide Substitution. The displacement reactions of dimethyl sulfoxide from complex **3** by 2,2′-bipyridine and 1,10-phenanthroline are represented in eq 6

$$cis\text{-}[Pt(Hbph)_2(dmso)_2] + N{-}N \rightarrow [Pt(Hbph)_2(N{-}N)] + 2dmso \quad (6)$$

The experiments were carried out in toluene at 298.2 ± 0.05 K. All reactions went to completion and obeyed a first-order rate law up to 90% conversion. A collection of the pseudo-first-order rate constants k_{obsd} for reaction 6, at various concentrations of entering diimine ligand (N−N = bpy, phen) and dimethyl sulfoxide, is reported in Tables S14 and S15. The kinetic data for the temperature dependence of the same reactions are given in Table S16.

In the absence of added free dimethyl sulfoxide, the pseudo-first-order plots show some deviation from linearity as the reaction proceeds, and dmso is generated from the complex. Deliberate addition of the nucleofuge (dmso) has a retarding effect on the rate, and the first-order plots become perfectly linear. At a constant sulfoxide concentration, a curvilinear dependence on the concentration of the entering nucleophile (bpy or phen) is observed which levels off to a limiting value at high concentration. A global 3-D representation of the [dmso] and [N−N] dependencies is given in Figure 5 for the substitution of *cis*-$[Pt(Hbph)_2(dmso)_2]$ by bpy in toluene at 298 K. The rate data appear to fit the nonlinear rate law

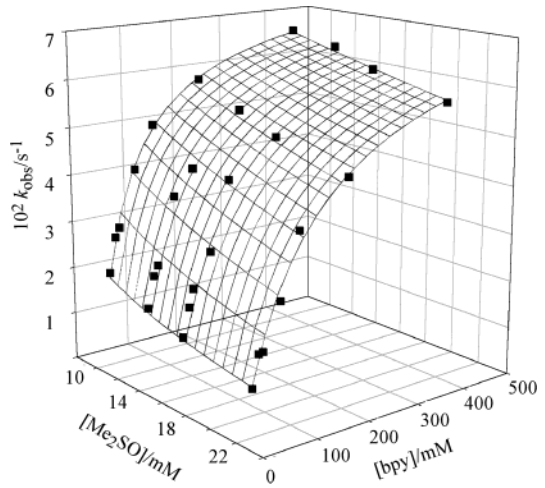

Figure 5. 3D-plot showing the dependence of the observed pseudo-first-order rate constants (k_{obsd}/s^{-1}) for reaction 6 (N−N = 2,2′ bipyridine) as a function of different amounts of entering ligand (bpy) and free dimethyl sulfoxide. (Experimental conditions: [dmso]/mM = 10.5; 14.0; 17.0; 22.4 in toluene at 298 K.)

$$k_{obsd} = a[N{-}N]/(b[dmso] + [N{-}N]) \quad (7)$$

The values of k_{obsd}, [N−N], and [dmso] were fitted to this expression using a nonlinear least-squares curve-fitting program,[46] and the best values of the constants a and b were obtained together with their standard deviations.

(iii) Dimethyl Sulfoxide Exchange. The kinetics of ligand exchange between coordinated and free dimethyl sulfoxide, see eq 8

$$cis\text{-}[Pt(Hbph)_2(dmso)_2] + 2dmso^* \rightarrow cis\text{-}[Pt(Hbph)_2(dmso^*)_2] + 2dmso \quad (8)$$

were investigated in chloroform-d or in toluene-d_8 as solvent by the ^{1}H NMR magnetization transfer technique. The calculated rate constants (k_{exch}/s^{-1}) are collected in Table S17. The ligand exchange was found to be independent of the concentration of added sulfoxide. A variable temperature study was undertaken for the calculations of the activation parameters.

Discussion

Atropisomerization and Intramolecular C−H Activation. The *cis*-bis(η^1-biphenyl) platinum derivatives **2**−**6** display static ^{1}H NMR spectra up to 333 K. No fluxional behavior was observed, and only one atropisomer was found in solution, suggesting restricted rotation about the Pt−C bond that preserves the head-to-tail conformation observed in the solid state for **5** and **6**.

Particularly useful for the identification of the atropisomer in solution were the results of phase-sensitive ^{1}H NOESY

(46) SCIENTIST, Micro Math Scientific Software, Salt Lake City, UT.

Chart 3

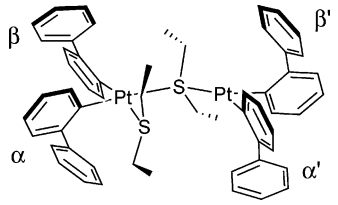

experiments and the strong through-space cross-peaks observed between hydrogen atoms of mutually cis Hbph groups. In particular, the predominance of a head-to-tail disposition of the two aryl groups is clearly indicated by strong nOe's cross-peaks between the $H_{8a,12a}$ protons on the pendant arm in one Ph−C fragment and the H_{3b} proton that lies on the phenyl ring opposite to it and directly coordinated in the cis position to the platinum(II) metal center. An additional consequence of the mutual interaction between pendant and coordinated aryl rings in a head-to-tail conformation is the marked anisotropic shift to low frequencies of the resonance of the *ortho*-protons $H_{3a,3b}$.

The high activation energy for atropisomerization of the *cis*-bis(η^1-biphenyl) platinum derivatives **2**−**6** is undoubtedly steric in origin. Similar steric effects are operative also in the dinuclear **1a** complex and are expected to be responsible for restricted Pt−C rotation as well. In this case, however, thioether bridge splitting, as depicted in Chart 3, can produce a relevant relief of steric congestion, allowing for a slow rotation of at least a pendant η^1-biphenyl fragment in the monobridged species.

Thus, atropisomerization of **1a** into **1b** could involve prior bridge splitting of the anterior thioether ligand (as seen in Chart 3) with rotation of the pendant α′ Hbph arm followed by bridge splitting of the posterior thioether and subsequent rotation of the β' organic fragment to afford the final $\alpha\beta\alpha\beta$ conformation of **1b**. Other sequences of bridge splitting and Pt−C rotation processes are conceivable which could involve, as a transient intermediate, the high energy $\alpha\beta\beta\beta$ species. The presence of this latter elusive component has been inferred by intense cross-peaks in the ^{1}H NOESY experiments (Figure 3) attributed to a fast exchanging species other than **1a**, **1b**, or the final cyclometalated complex. The same experiments showed the occurrence of chemical exchange on the NMR time-scale between ethyl groups belonging to the same sulfur atom which imply preliminary bridge splitting and subsequent inversion of configuration at the uncoordinated sulfur atom.

Thioether dissociation seems to be also at the origin of the intramolecular C−H activation that leads to the formation of the cyclometalated $[Pt_2(bph)_2(\mu\text{-}SEt_2)_2]$ compound. The most conceivable mechanism involves preliminary bond dissociation at a thioether bridge, as depicted in Chart 3. The dinuclear $[Pt_2(Hbph)_4(\mu\text{-}SEt_2)_2]$ compound exhibits the same propensity to dissociation as found by Puddephatt for $[Pt_2Me_4(\mu\text{-}SMe_2)_2]$[19] as a precursor to platinum compounds containing bidentate (C,N) or terdentate (C,N,N′) ligands.[47] Dissociation of the Pt−S bond on **1b** originates coordinative and electronic unsaturation at a single metal atom (three-coordinate, 14-electron species). The behavior observed is also consistent with a preequilibrium in which a molecule of dimer gives two 14-electron T-shaped monomers:

$$[Pt_2(Hbph)_4(\mu\text{-}SEt_2)_2] \leftrightarrows 2[Pt(Hbph)_2(SEt_2)] \qquad (9)$$

The monomeric species $[Pt(Hbph)_2(SEt_2)]$ might be stabilized by an agostic interaction involving the empty σ orbital on Pt and the electron pair of the C−H bond at the C_{8a} or the C_{12a} sites. This hypothesis is strongly supported by the observation that bulky ligands favor the formation of agostic interactions between the metal and C−H bonds[48] and that cyclometalation is initiated by an agostic interaction with the σ(C−H) orbital followed by back-donation to the σ^*(CH) orbital.[49] It might be claimed that the transient agostic $[Pt(Hbph)_2(SEt_2)]$ should be considered a 16-electron species. We will turn our attention to this problem later, when discussing the characteristics of three-coordinate d^8 species as reaction intermediates or structurally characterized compounds. Right now, we observe that the 16-electron full four-coordinate monomers *cis*-$[Pt(Hbph)_2(SEt_2)_2]$ or *cis*-$[Pt(Hbph)_2(dmso)_2]$ complexes do not undergo cyclometalation under the same conditions illustrated above for the dinuclear $[Pt_2(Hbph)_4(\mu\text{-}SEt_2)_2]$ compound. Oxidative addition of the C−H bond at the $C_{8a,12a}$ sites follows this preliminary Pt−CH interaction, yielding a cyclometalated-arylhydrido 16-electron Pt(IV) five-coordinate intermediate. Several theoretical studies have indicated that these reaction intermediates should have square-pyramidal geometry,[50] but only recently have two papers appeared describing the isolation and structural characterization of such compounds.[51] Finally, reductive elimination should yield the dinuclear cyclometalated species $[Pt_2(bph)_2(\mu\text{-}SEt_2)_2]$ and free biphenyl. Cyclometalation on **1b** develops along the same key steps recognized by the Whitesides' group for $[Pt(PEt_3)_2(CH_2CMe_3)_2]$:[52] (i) reversible dissociation of the phosphane ligand, (ii) oxidative addition of the C−H bond to the coordinatively unsaturated intermediate, (iii) rate-limiting reductive elimination of neopentane, and (iv) reassociation of triethylphosphane. The reason why intramolecular C−H activation exhibits a higher energy barrier in **1a** ($\alpha\beta\beta\alpha$ conformation) than in **1b** ($\alpha\beta\alpha\beta$) is still not clear. We are inclined to think that in the latter conformation the equilibrium of eq 9 is more shifted toward the couple of monomers where the $C-H_{8a,12a}$ bonds of the noncoordinated phenyl fragment have easy access to the vacant coordination site on the metal. The good computer-fit of the kinetic data in Figure 4 does not exclude that the proposed unsaturated intermediate for metalation should be to some extent reached also from **1a**.

Dissociative Exchange and Substitution. The exchange of the coordinated dmso in compound **3** with free ligand in toluene-

(47) (a) Anderson, C. M.; Crespo, M.; Jennings, M. C.; Lough, A. J.; Ferguson, G.; Puddephatt, R. J. *Organometallics* **1991**, *10*, 2672−2679. (b) Crespo, M.; Martinez, M.; Sales, J.; Solans, X.; Font-Bardía, M. *Organometallics* **1992**, *11*, 1288−1295.

(48) (a) Brookhart, M.; Green, M. L. H. *J. Organomet. Chem.* **1983**, *250*, 395−408. (b) Cotton, F. A.; LaCour, T.; Stanislowski, A. G. *J. Am. Chem. Soc.* **1974**, *96*, 754−760.

(49) (a) Crabtree, R. H.; Holt, E. M.; Lavin, M.; Morehouse, S. M. *Inorg. Chem.* **1985**, *24*, 1986−1992. (b) Lavin, M.; Crabtree, R. H. *Organometallics* **1989**, *8*, 99−104.

(50) (a) Hill, G. S.; Puddephatt, R. J. *Organometallics* **1998**, *17*, 1478−1486. (b) Siegbahn, P. E. M.; Crabtree, R. H. *J. Am. Chem. Soc.* **1996**, *118*, 4442−4450. (c) Bartlett, K. L.; Goldberg, K. I.; Borden, W. T. *J. Am. Chem. Soc.* **2000**, *122*, 1456−1465. (d) Bartlett, K. L.; Goldberg, K. I.; Borden, W. T. *Organometallics* **2001**, *20*, 2669−2678. (e) Heiberg, H.; Johansson, L.; Gropen, O.; Ryan, O. B.; Swang, O.; Tilset, M. *J. Am. Chem. Soc.* **2000**, *122*, 10831−10845. (f) Gilbert, T. M.; Hristov, I.; Ziegler, T. *Organometallics* **2001**, *20*, 1183−1189.

(51) (a) Fekl, U.; Kaminsky, W.; Goldberg, K. I. *J. Am. Chem. Soc.* **2001**, *123*, 6423−6424. (b) Reinartz, S.; White, P. S.; Brookhart, M.; Templeton, J. L. *J. Am. Chem. Soc.* **2001**, *123*, 6425−6426.

(52) Foley, P.; DiCosimo, R.; Whitesides, G. M. *J. Am. Chem. Soc.* **1980**, *102*, 6713−6725.

Scheme 2

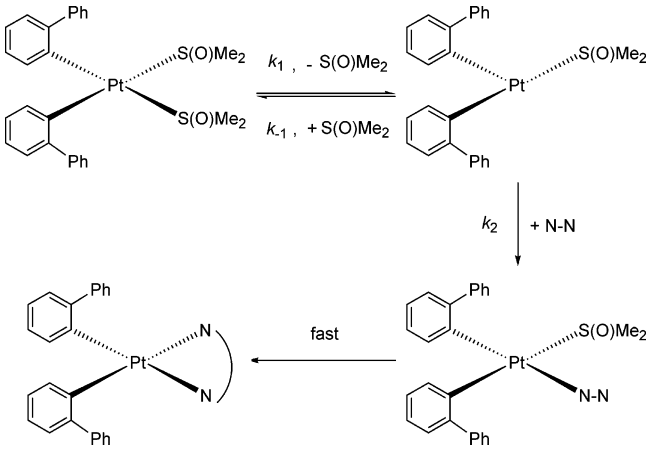

d_8 (eq 8) takes place with a rate law of the form rate = k_{exch}[complex], with $k_{exch} = (114 \pm 3) \times 10^{-3}$ s^{-1} at 298 K.[53] There is no sulfoxide-dependent contribution, even at the highest sulfoxide concentrations. The temperature dependence of k_{exch} gives $\Delta H^{\ddagger} = (95 \pm 3)$ kJ mol^{-1} and $\Delta S^{\ddagger} = (56 \pm 10)$ J K^{-1} mol^{-1}. As expected for dissociatively activated processes, the entropy of activation is positive. The exchange rate constant at 298 K and the activation parameters in $CDCl_3$ are as follows: $k_{exch} = (288 \pm 8) \times 10^{-3}$ s^{-1}, $\Delta H^{\ddagger} = (93 \pm 5)$ kJ mol^{-1}, and $\Delta S^{\ddagger} = (56 \pm 17)$ J K^{-1} mol^{-1}. Such differences may be due to the different solvating power of toluene and chloroform.

Proton NMR and electronic spectra clearly indicate that the reaction of *cis*-[Pt(Hbph)$_2$(dmso)$_2$] with 2,2′-bipyridine and 1,10-phenanthroline according to eq 6 occurs in a single observable stage, ring closing being much faster than displacement of the first dmso, and is retarded by the addition of free dmso. The pattern is strictly similar to that found in our previous studies on *cis*-[Pt(C,C)(S,S)] (S = thioethers or sulfoxides) systems where the easy dissociation of the ligand S was shown to be the rate-determining step of the substitution. The same dissociative mechanism (Scheme 2) applies which involves: (i) dissociative loss of dmso from the substrate (k_1 path) to yield a three-coordinated 14-electron intermediate, and (ii) competition for it between the re-entry of dmso (via k_{-1}) and the attack of a ligand (either dmso* or N−N, via k_2) to yield the observed products. The rate law is given by the equation:

$$k_{obsd} = k_1[\text{N}-\text{N}]/\{(k_{-1}/k_2)[\text{dmso}] + [\text{N}-\text{N}]\} \qquad (10)$$

that reduces to $k_{obsd} = k_1$ for $k_2 \gg k_{-1}$. The rate constants are related to the empirical parameters a and b in eq 7 by the expressions $a = k_1$ and $b = k_{-1}/k_2$. The dissociation constant k_1 measures the rate of sulfoxide leaving the coordination sphere of the metal, while the k_2/k_{-1} ratio measures the competition between N−N and the leaving sulfoxide for the three-coordinate intermediate. Rate constants and activation parameters derived from the kinetic analysis of nucleophilic substitution of *cis*-[Pt(Hbph)$_2$(dmso)$_2$] with bpy [$k_1 = (76 \pm 1) \times 10^{-3}$ s^{-1}, $\Delta H^{\ddagger} = (84 \pm 1)$ kJ mol^{-1}, $\Delta S^{\ddagger} = (15 \pm 3)$ J K^{-1} mol^{-1}, in toluene at 298 K] and with phen [$k_1 = (78 \pm 2) \times 10^{-3}$ s^{-1}, $\Delta H^{\ddagger} = (78 \pm 3)$ kJ mol^{-1}, $\Delta S^{\ddagger} = (-5 \pm 9)$ J K^{-1} mol^{-1}] are substantially identical and comparable to those obtained from the kinetics of ligand exchange, within the experimental error.

The experimental kinetic evidence points unequivocally to a dissociative mode of activation (D, according to the Langford−Gray nomenclature)[3f] for the system here examined. The assessment of a dissociative mechanism is accredited by: (i) the dissociation rate k_1 being independent of the nature and concentration of the entering group N−N, (ii) the rate of dmso dissociation k_1 being independent of the nature of N−N and substantially identical to the rate constant k_{exch} for dmso exchange, (iii) the mass-law retardation plots suggesting a competition between the nucleofuge dmso and the nucleophile N−N for an intermediate of a lower coordination number; the intermediate has a lifetime long enough to discriminate between different entering groups ($k_2/k_{-1} = 0.18$ for bpy and 0.621 for phen, respectively), and (iv) the magnitude of the positive entropy of activation. The solvents used have an insufficiently coordinating power to give an associatively activated contribution. Accordingly, a study on the pressure dependence of ligand exchange rate constants of similar complexes, including *cis*-[PtPh$_2$(dmso)$_2$], in nonpolar solvents, led to positive values of the activation volumes.[26]

It is of interest to focus shortly on some attractive features emerging from the comparison of the kinetic data in Table 5 of compounds exhibiting a dissociative behavior. The change from CH_3 (entry 1, $k_{exch} = 0.0112$ s^{-1}) to C_6H_5 (entry 2, $k_{exch} = 0.0140$ s^{-1}) does not greatly affect the dissociative activation. Inductive σ effects are dominant, the extent of the aryl−platinum π interaction being small. The stabilization of the three-coordinate intermediate by interaction between Pt and the phenyl hydrogens in [PtPh$_2$(dmso)] plays little, if any, part in promoting the dissociative nature of the process. The dissociative mechanism is expected to be enhanced by extra electron release from the ligands, but changing from C_6H_5 to *4*-$CH_3C_6H_4$ (entry 3) leads to no significant change in the magnitude of k_l. A pentafluorophenyl group (entry 4) in place of the phenyl group induces a significant decrease of lability. Because molecular structures of similar compounds show that phenyl and pentafluorophenyl groups exert a comparable trans influence,[54] there are no arguments to suggest that this result may be ascribed to a ground-state effect, that is, to the strength of the Pt−S bond. Rather, it seems that a ligand-to-metal reduction of electron density brings about a noticeable destabilization of the three-coordinated intermediate. Substitution in the complex containing the planar 2,2′-biphenyl dianion (entry 7) is still dissociative and largely easier than in its analogue containing single aryl ligands (entry 6), despite its presumed π-acceptor properties. It must be concluded that back-donation from filled d orbitals to empty π^* of the in-plane cyclometalated rings is weak or absent and is not operative in promoting a changeover from dissociative to associative mode of activation. The complex *cis*-[Pt(Hbph)$_2$(dmso)$_2$] (entry 5), despite the remarkable steric congestion of the two noncoordinated aryl groups lying above and below the coordination plane in a "pseudo-octahedral" fashion, reacts at a similar rate as the planar [Pt(bph)(Me$_2$S)$_2$] (entry 7). Finally, the reactivity appears to be sensitive to the electron-donating ability of the substituents on the sulfur atom of the leaving group

(53) Derived from the Eyring plot.

(54) Bresciani Pahor, N.; Plazzotta, M.; Randaccio, L.; Bruno, G.; Ricevuto, V.; Romeo, R. *Inorg. Chim. Acta* **1978**, *31*, 171−175.

Table 5. Selected Kinetic Data for Dissociation of Ligands from Pt(II) Complexes at 303 K

	complex	solvent	ligand	10^3k_{exch} [a]	10^3k_1 [b]	(k_2/k_{-1}) [c]	$\Delta V^{\ddagger}$ [d]	ref
1	*cis*-$[Pt(Me)_2(dmso)_2]$	benzene	dmso	21[e]	11.2	0.17	+4.9	26, 29
2	*cis*-$[Pt(Ph)_2(dmso)_2]$	benzene	dmso	79[f]	14.0	0.049	+5.5	26, 30
3	*cis*-$[Pt(p\text{-tolyl})_2(dmso)_2]$	benzene	dmso		15.9	0.044		30
4	*cis*-$[Pt(C_6F_5)_2(dmso)_2]$	toluene	dmso		0.89	0.055		31
5	*cis*-$[Pt(Hbph)_2(dmso)_2]$	toluene	dmso	220[e]	140	0.18		this work
6	*cis*-$[Pt(Ph)_2(Me_2S)_2]$	benzene	Me_2S	3.8[e]	5.3	0.68	+4.7	26, 28
7	$[Pt(bph)(Me_2S)_2]$	toluene	Me_2S		107[g]	0.096		25
		chloroform		1060[g]				
8	$[Pt(bph)(Et_2S)_2]$	toluene	Et_2S		30[g]	0.46		25
		chloroform		84[g]				
9	*cis*-$[Pt(Me)_2(dmso)(PPh_3)]$	chloroform	dmso	114[e]	114[e]			32
10	*cis*-$[Pt(MePh_2Si)_2(Me_2PhP)_2]$	toluene	Me_2PhP	56				33

[a] In s^{-1}, from magnetization transfer experiments. [b] In s^{-1}, from substitution reaction studies with bpy. [c] Competition ratio. [d] Activation volume in cm^3. [e] Calculated from the Eyring equation. [f] By flow ^1H NMR. [g] At 298 K.

(cf. entries 7 and 8), in agreement with previous findings on a series of compounds of the type *cis*-$[PtPh_2L_2]$,[27] where L encompasses a wide range of thioethers of different electron-donating characteristics.

Three-Coordinate Intermediates. This work has confirmed that a ligand set of two cis σ-bonded carbon atoms and two sulfur atoms induces dissociation of one of the sulfur ligands, no matter whether the carbon atom comes from an alkyl, an aryl, or a metalated aryl ligand. Cyclometalation and in-plane disposition of aryl rings do not favor an associative pathway, through the increase of electrophilicity of the platinum center, because the expected back-donation toward the aromatic π^* orbitals does not come into play. The low-energy dissociative pathway is therefore a combined result of: (i) the presence of a high electronic barrier at the metal which prevents the approach of the nucleophile lone-pair, (ii) bond weakening at the leaving group due to the trans influence of strong σ-donors (in the present cases, the organic carbanions which form strong Pt−C σ-bonds), and (iii) the stabilization of the remaining set of three in-plane ligands in a T-shaped structure which allows the 14-electron intermediate to maintain the original singlet ground state. These favorable electronic factors still apply to *cis*-$[PtMe_2(PPh_3)(dmso)]$ (entry 9 in Table 5), where the introduction of the σ-donor PR_3 produces no changeover of mechanism or does not greatly affect the easily achieved dissociative activation. The same reasoning applies to the tetrahedral distorted Werner-type compound *cis*-$[Pt(MePh_2Si)_2(Me_2PhP)_2]$ (entry 10), where an appropriate set of strong σ-donor silyl groups can favor sufficient accumulation of electron density at the metal and stabilization of the 14-e intermediate. If one of the thioethers is displaced by CO, as in *cis*-$[PtPh_2(CO)(SMe_2)]$,[34] the mechanism changes again from a dissociative to an associative one, as discussed previously.

Once the main features to induce dissociation on a four-coordinate d^8 metal complex have been recognized, one starts to wonder to what extent the knowledge gained in mechanistic studies can be exploited for synthetic purposes. We know we must deal with electron-rich four-coordinate complexes. The value of the dissociation rate constant is an indication of the ease with which the bond breaking process occurs and of stabilization of the three-coordinate intermediate. The competition ratio between nucleofuge and nucleophile measures the discrimination ability of the intermediate and its lifetime. Molecular orbital calculations suggest that three-coordinate 14-e d^8-ML_3 species have a T-shaped geometry, but the concentration of this intermediate in solution is always very low and the possibility of detecting it with spectroscopic techniques is a hard, or impossible, task. The coordinative and electronic unsaturation increases enormously the electrophilicity of the intermediate and its tendency to coordinate solvent molecules or any other electron-donating moiety, including the electron pair of a C−H bond (agostic interaction) or electrons coming from a donor atom of noninnocent ligands. Interactions of this type are of greatest importance in the approach to the isolation and structural characterization of such three-coordinate species, having in mind, however, that the stabilization of transient species generated in situ by ligand dissociation is reflected in a sharp increase of reactivity.

The β-Hydrogen Kinetic Effect. Orpen and Spencer[55] have described the structure of β-agostic cationic platinum(II) complexes of the type $[Pt(P{-}P)(R)]^+$ (P−P = chelating diphosphane; R = alkyl), where the chelating ligand prevents isomerization and the platinum interaction with a β-hydrogen of the alkyl group is so extended as to favor the formation of a well-defined 3-center-2-electron Pt−H−C bond. The same structure can be envisaged for the three-coordinate transition state formed upon solvent dissociation in the uncatalyzed cis to trans isomerization[16a] of *cis*-$[Pt(PEt_3)_2(R)(S)]^+$ (R = linear or branched alkyls; S = MeOH). In these solvento complexes, when R = Et, *n*-Pr, *n*-Bu, the rate of isomerization is much higher than that of complexes containing alkyl groups with no β-hydrogen atoms, such as methyl, neopentyl, and trimethylsilyl groups. Inductive or steric effects cannot account for the large β-hydrogen kinetic effect. A specific interaction of these hydrogen atoms with the metal is likely to be responsible for the large rate enhancement. The extent of Pt−H interaction in the *cis*-$[Pt(PEt_3)_2(Et)]^+$ transition state is presumably less than in the structurally characterized $[Pt(P{-}P)(Et)]^+$, but it is sufficient to partly satisfy the coordinative unsaturation, to decrease its energy, and to accelerate the fluxionality of the intermediate. A tentative calculation of the free energy involved in the β-hydrogen kinetic effect can be performed, based on the reasonable assumption that the relative ground-state energies of the square-planar *cis*-$[Pt(PEt_3)_2(Me)(S)]^+$ and *cis*-$[Pt(PEt_3)_2(Et)(S)]^+$ complexes are not greatly different. The free energy of activation for the methyl solvento complex is 87.2 kJ mol^{-1}, whereas that for the ethyl complex is 63.4 kJ mol^{-1}. The difference between these two values should reflect entirely the

(55) Carr, N.; Mole, L.; Orpen, A. G.; Spencer, J. L. *J. Chem. Soc., Dalton Trans.* **1992**, 2653−2662. (b) Mole, L.; Spencer, J. L.; Carr, N.; Orpen, A. G. *Organometallics* **1991**, *10*, 49−52.

Chart 4

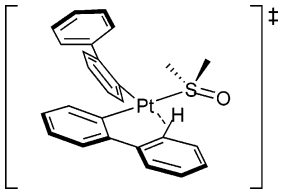

free energy involved in the β-hydrogen kinetic effect. This effect has consequences on the rates of dissociative processes that parallel the spectroscopic and structural properties of structurally characterized compounds with full β-agostic interactions such as $[Pt(P-P)(Et)]^+$. If steric effects play little, if any, role in promoting dissociation (compare in Table 5 the reactivity of the highly congested *cis*-$[Pt(Hbph)_2(dmso)_2]$ and the flat planar $[Pt(bph)(Me_2S)_2]$), then the rate acceleration exhibited by *cis*-$[Pt(Hbph)_2(dmso)_2]$ (entry 5) with respect to *cis*-$[Pt(Ph)_2(dmso)_2]$ (entry 2) can be attributed to hydrogen interactions in the transition state of the type described in Chart 4. These hydrogen interactions, while lowering the energy of the TS below that of a formally three-coordinate 14-electron species (by only 8.4 kJ mol^{-1}, as derived from the rate data in Table 5), are insufficiently stabilizing to allow such species to be isolated and characterized. An alternative explanation, kinetically indistinguishable from the stabilization of the TS, could involve steric congestion in the ground state and a direct participation of the dangling *ortho*-phenyl substituents in promoting steric relief and easier removal of dmso, even though little bond distortion is to be expected on going from a four-coordinate square-planar arrangement to a T-shaped three-coordinate geometry. It is possible that both effects, steric and electronic, come contemporarily into play, within the framework of a dissociative substitution.

A survey of the X-ray data on a few isolated three-coordinate 14-e d^8-ML_3 species shows C−H bonds involved in agostic interactions to the empty coordination site of otherwise T-shaped d^8 complexes. These examples include the anion[56] $[Ni(mesityl)_3]^-$, the cation[57] $[Rh(PPh_3)_3]^+$, the very recent $[Rh(Bu_2^tPCH_2PBu_2^t)(np)]$[58] (np = neopentyl), and $[PdArX(PBu^t_2R)]$ (Ar = Ph, X = Br, R = adamantyl; Ar = 2,4-xylyl, X = I, R = Bu^t).[59] Agostic interactions stabilize also the novel "T-shaped 14-electron" platinum(II) cations *trans*-$[Pt(CH_3)L_2]^+$ [L = PR_2-(2,6-$Me_2C_6H_3$), R = Ph, Cy].[60] A formally three-coordinate cationic complex $[Pd(CH_2CMe_2Ph)(dmpe)]^+$ appears to be stabilized by an auxiliary π, η^1 interaction with the *ipso*-carbon of the phenyl group.[61]

Espinet[11c] argues strongly against such species being considered three-coordinate 14-electron species. However, the challenge to isolate "14-electron T-shaped" compounds and to confirm their structures experimentally, according to what is discussed above and to the characteristics of the few structurally characterized compounds so far, relies on the use of ligands that guarantee some form of protection of the fourth coordination site and of electron transfer to the vacant σ orbital of the metal. To what extent such electron transfer occurs can be a matter of debate, but essential is the knowledge acquired from kinetic studies to detect new synthetic procedures and to explore the role of these fascinating elusive species in fundamental processes such as C−H bond activation, hydroformylation, or polymerization reactions.

Conclusion

The chemistry of the novel dinuclear compound $[Pt_2(\mu\text{-}SEt_2)_2(Hbph)_4]$, **1a**, appears to be complex and intriguing. The presence of pendant η^1-biphenyl groups determines an interesting atropisomerization between two preferential low-energy conformations and the intramolecular C−H activation leading to cycloplatination. Opening of the thioether bridge and formation of a coordinatively unsaturated species is a prerequisite for the occurrence of both processes. By analogy with well-known dinuclear species, such as $[Pt_2(\mu\text{-}SEt_2)_2(C_6H_5)_4]$[62] and $[Pt_2(\mu\text{-}SMe_2)_2(Me)_4]$,[19,63] **1a** can be exploited as a synthetic precursor to a large variety of organometallic species containing the $[Pt(Hbph)_2]$ moiety. Two such compounds, with 2,2′-bipyridine and 1,10-phenanthroline, have been structurally characterized by X-ray diffraction studies. A detailed kinetic study of ligand (dmso) exchange and substitution (by 2,2′-bipyridine and 1,10-phenanthroline), performed on the novel complex *cis*-$[Pt(Hbph)_2(dmso)_2]$, has confirmed that a ligand set of two cis σ-bonded carbon atoms and two sulfur atoms induces dissociation of one of the sulfur ligands, no matter whether the carbon atom comes from an alkyl, an aryl, or a metalated aryl ligand. The new data allow for an updated understanding of the factors controlling the changeover from associative to dissociative pathways in square-planar d^8 metal complexes. The question is addressed at what extent the knowledge gained in mechanistic studies on ML_3 d^8 T-shaped 14-electron species can be exploited for synthetic purposes. It is pointed out that, when such species have been isolated and structurally characterized, they show C−H bonds being involved in agostic interactions with the metal center. These interactions guarantee some form of protection of the fourth coordination site and electron transfer to the vacant σ orbital of the metal. When occurring within a transition state or a three-coordinate intermediate, it is classified as the β-hydrogen kinetic effect, presumably leading to a sharp increase of the ligand dissociation rate.

Experimental Section

General Procedures and Chemicals. All syntheses were performed on a double-manifold Schlenk vacuum line under a dry and oxygen-free dinitrogen atmosphere using freshly distilled, dried, and degassed solvents. Solvents employed in the synthetic procedures (Analytical Reagent Grade, Lab-Scan, Ltd.) and in the kinetic runs (A.C.S. spectrophotometric grade, Aldrich Chem. Co.) were distilled under dinitrogen from sodium-benzophenone ketyl (tetrahydrofuran, diethyl ether, toluene) or barium oxide (dichloromethane).[64] Chloroform-*d* (99.8

(56) Hay-Motherwell, R.; Wilkinson, G.; Sweet, T. K. N.; Hursthouse, M. B. *Polyhedron* **1996**, *15*, 3163−3166.
(57) Yared, Y. W.; Miles, S. L.; Bau, R.; Reed, C. A. *J. Am. Chem. Soc.* **1977**, *99*, 7076−7078.
(58) Urtel, H.; Meier, C.; Eisenträger, F.; Rominger, F.; Joschek, J. P.; Hofmann, P. *Angew. Chem., Int. Ed.* **2001**, *40*, 781−784.
(59) Stambuli, J. P.; Bühl, M.; Hartwig, J. F. *J. Am. Chem. Soc.* **2002**, *124*, 9346−9347.
(60) Baratta, W.; Stoccoro, S.; Doppiu, A.; Herdtweck, E.; Zucca, A.; Rigo, P. *Angew. Chem., Int. Ed.* **2003**, *42*, 105−108.
(61) Campora, J.; Gutiérrez-Puebla, E.; López, J. A.; Monge, A.; Palma, P.; del Río, D.; Carmona, E. *Angew. Chem., Int. Ed.* **2001**, *40*, 3641−3644.
(62) Steele, B. R.; Vrieze, K. *Transition Met. Chem.* **1977**, *2*, 140−144.
(63) (a) Rashidi, M.; Hashemi, M.; Khorasani-Motlagh, M.; Puddephatt, R. J. *Organometallics* **2000**, *19*, 2751−2755. (b) Rashidi, M.; Fakhroeian, Z.; Puddephatt, R. J. *J. Organomet. Chem.* **1991**, *406*, 261−267.
(64) Riddick, J. A.; Bunger, W. B.; Sakano, T. K. In *Organic Solvents*, 4th ed.; Weissberger, A., Ed.; Wiley & Sons: New York, 1986.

+ %, C.I.L., Inc.) and toluene-d_8 (99 + %, Aldrich Chem. Co.) were used as received. Dimethyl sulfoxide was purified by filtration through a 2 × 25 cm chromatographic column filled with alumina (activated grade I, neutral, 150 mesh, Aldrich), under a dinitrogen atmosphere. All of the other reagents were purchased from commercial suppliers and used without further purification. Elemental analyses were performed by Redox SNC (Milan, Italy).

Synthesis of Complexes. Complexes *cis*-[$PtCl_2(SEt_2)_2$][65] and [PtI_2(COD)][66] were synthesized following the procedures reported in the literature.

[$Pt_2(\mu$-$SEt_2)_2$(Hbph)$_4$], 1a (Hbph$^-$ = η^1-2,2′-biphenyl anion), was obtained adventitiously as a side product in the course of the synthesis of the dinuclear cyclometalated species [$Pt_2(\mu$-$SEt_2)_2$(bph)$_2$] according to the procedure reported by von Zelewsky et al.[35] A solution of 2,2′-Li_2bph in ethyl ether[67] (40 mL, 0.135 M) was added dropwise to a stirred suspension of *cis*-[$PtCl_2(SEt_2)_2$] (1.2 g, 2.69 mmol) in 40 mL of diethyl ether at −10 °C. The reaction mixture was kept for 1 h at −10 °C, subsequently warmed to 0 °C, kept for an additional hour at this temperature, and then hydrolyzed with 20 mL of water. The organic phase was separated out, and the residual product was extracted from the aqueous solution with dichloromethane (4 × 10 mL); the CH_2Cl_2 extract was combined with the original organic fraction and left overnight over Na_2SO_4. After evaporation to dryness, the residue was dissolved in the minimum amount of dichloromethane. Chromatography over a 2 × 20 cm silica gel column with a mixture of dichloromethane/hexane (3/2 = v/v) afforded 200 mg of the dinuclear complex [$Pt_2(\mu$-$SEt_2)_2$(bph)$_2$] (17% yield) from the yellow band, isolated by recrystallization from dichloromethane/pentane (1/1 = v/v). Collection of the colorless initial fractions before the yellow band and subsequent workup according to the procedure described above afforded the dinuclear uncyclometalated species [$Pt_2(\mu$-$SEt_2)_2$(Hbph)$_4$] (**1a**) as a crystalline off-white solid (300 mg, 19% yield). Anal. Calcd for $C_{56}H_{56}Pt_2S_2$: C, 56.8; H, 4.8; S, 5.4. Found: C, 56.1; H, 4.9; S, 5.3. ^{1}H NMR ($CDCl_3$): δ 7.61 (d, br, 8H, $H_{8a,12a}$+$H_{8b,12b}$), 7.41 (m, br, 12H, $H_{9a,11a}$+$H_{9b,11b}$+$H_{10a,10b}$), 6.84 (dd, $^3J_{HH}$ = 7.5 Hz, $^4J_{HH}$ = 1.4 Hz, 4H, $H_{6a,6b}$), 6.71 (dd, $^3J_{av}$ = 7.1 Hz, 4H, $H_{5a,5b}$), 6.52 (dd, $^3J_{av}$ = 7.3 Hz, 4H, $H_{4a,4b}$), 6.28 (d, $^3J_{HH}$ = 7.2 Hz, $^3J_{PtH}$ = 71.0 Hz, 4H, $H_{3a,3b}$), 2.69 (m, br, 4H, S−CH_{2b}−CH_3), 2.67 (m, br, 4H, S−CH_{2a}−CH_3), 2.00 (t, $^3J_{HH}$ = 7.1 Hz, 6H, S−CH_2−CH_{3a}), 0.288 (t, $^3J_{HH}$ = 7.2 Hz, 6H, S−CH_2−CH_{3b}). ^{13}C{^{1}H} NMR ($CDCl_3$, T = 273 K): δ 135.7 ($C_{3a,3b}$), 129.7 ($C_{8a,12a}$+$C_{8b,12b}$), 128.8 ($C_{6a,6b}$), 127.2 ($C_{9a,11a}$+$C_{9b,11b}$), 125.8 ($C_{10a,10b}$), 125.2 ($C_{4a,4b}$), 122.2 ($C_{5a,5b}$), 33.1 (S−CH_{2b}−CH_3), 22.8 (S−CH_{2a}−CH_3), 11.9 (S−CH_2−CH_{3a}), 9.51 (S−CH_2−CH_{3b}).

^{1}H NMR spectrometry in $CDCl_3$ showed compound **1a** to evolve with time toward the conformer **1b**, which was separated almost quantitatively from **1a** by several subsequent crystallizations from a dichloromethane/petroleum ether mixture (1/1 = v/v).

[$Pt_2(\mu$-$SEt_2)_2$(Hbph)$_4$], 1b. ^{1}H NMR ($CDCl_3$): δ 7.58 (d, br, $^3J_{HH}$ = 7.7 Hz, 8H, $H_{8a,12a}$+$H_{8b,12b}$), 7.43 (m, br, $^3J_{HH}$ = 7.7 Hz, 8H, $H_{9a,11a}$+$H_{9b,11b}$), 7.33 (m, br, $^3J_{HH}$ = 7.7 Hz, 4H, $H_{10a,10b}$), 6.94 (dd, $^3J_{HH}$ = 7.7 Hz, 4H, $H_{6a,6b}$), 6.81 (dd, $^3J_{av}$ = 7.7 Hz, 4H, $H_{5a,5b}$), 6.64 (dd, $^3J_{av}$ = 7.3 Hz, 4H, $H_{4a,4b}$), 6.48 (d, $^3J_{HH}$ = 7.3 Hz, $^3J_{PtH}$ = 69.0 Hz, 4H, $H_{3a,3b}$), 3.40 (m, br, $^3J_{HH}$ = 7.9 Hz, 2H, S−CH_{2a}−CH_3), 3.19 (m, br, $^3J_{HH}$ = 7.7 Hz, 2H, S−CH_{2b}−CH_3), 2.94 (m, br, $^3J_{HH}$ = 7.9 Hz, 2H, S−C$H_{2a'}$−CH_3), 2.88 (m, br, $^3J_{HH}$ = 7.7 Hz, 2H, S−C$H_{2b'}$−CH_3), 1.83 (t, $^3J_{HH}$ = 7.9 Hz, 6H, S−CH_2−CH_{3a}), 1.30 (t, $^3J_{HH}$ = 7.7 Hz, 6H, S−CH_2−CH_{3b}). ^{13}C{^{1}H} NMR ($CDCl_3$): δ 136.1 ($C_{3a,3b}$), 129.2 ($C_{6a,6b}$), 128.8 ($C_{9a,11a}$+$C_{9b,11b}$), 127.2 ($C_{8a,12a}$+$C_{8b,12b}$), 127.0 ($C_{10a,10b}$), 125.3 ($C_{4a,4b}$), 122.5 ($C_{5a,5b}$), 33.7 (S−CH_{2b}−CH_3), 33.3 (S−C$H_{2b'}$−CH_3), 30.5 (S−CH_{2a}−CH_3), 30.3 (S−C$H_{2a'}$−CH_3), 12.9 (S−CH_2−CH_{3a}), 12.5 (S−CH_2−CH_{3b}).

[Pt(Hbph)$_2$(COD)], 2. A suspension of [PtI_2(COD)] (200 mg, 0.36 mmol) in diethyl ether (20 mL) was cooled at −10 °C and treated with 2,2′-Li_2bph (5.4 mL, 0.135 M) in diethyl ether. The mixture was stirred for 2 h while being warmed to room temperature and then worked up with 10 mL of water. After extraction of the aqueous solution with dichloromethane, the combined organic extracts were dried over sodium sulfate and filtered off. Evaporation of the solvent under reduced pressure and recrystallization from toluene/petroleum ether (1/1 v/v) gave **2** as an off-white solid (170 mg, 78%). Anal. Calcd for $C_{32}H_{30}Pt$: C, 63.0; H, 4.9. Found: C, 63.5; H, 4.8. ^{1}H NMR ($CDCl_3$): δ 7.44 (m, 4H, $H_{8a,12a}$+$H_{8b,12b}$), 7.33 (m, 6H, $H_{9a,11a}$+$H_{9b,11b}$+$H_{10a,10b}$), 6.93 (dd, $^4J_{PtH}$ = 26.4 Hz, $^3J_{HH}$ = 7.2 Hz, $^4J_{HH}$ = 1.1 Hz, 2H, $H_{6a,6b}$), 6.76 (ddd, $^3J_{av}$ = 7.2 Hz, $^4J_{HH}$ = 1.1 Hz, 2H, $H_{5a,5b}$), 6.64 (ddd, $^4J_{PtH}$ = 13.8 Hz, $^3J_{av}$ = 7.2 Hz, $^4J_{HH}$ = 1.1 Hz, 2H, $H_{4a,4b}$), 6.20 (d, $^3J_{PtH}$ = 69.3 Hz, $^3J_{HH}$ = 7.2 Hz, 2H, $H_{3a,3b}$), 5.05 (m, br, $^2J_{PtH}$ = 42.8 Hz, 2H, $CH_{1,5}$), 4.81 (m, br, $^2J_{PtH}$ = 39.2 Hz, 2H, $CH_{2,6}$), 2.46+2.36 (m, br, 4H, $(CH_2)_{4,8}$), 2.30 (m, br, 4H, $(CH_2)_{3,7}$). ^{13}C{^{1}H} NMR ($CDCl_3$): δ 151.4 ($^1J_{PtC}$ = 1117 Hz, $C_{2a,2b}$), 148.0 ($^2J_{PtC}$ = 39 Hz, $C_{1a,1b}$), 146.6 ($^3J_{PtC}$ = 34 Hz, $C_{7a,7b}$), 136.2 ($^2J_{PtC}$ = 14 Hz, $C_{3a,3b}$), 129.7 ($C_{8a,12a}$+$C_{8b,12b}$), 129.0 ($^3J_{PtC}$ = 59 Hz, $C_{6a,6b}$), 127.1 ($C_{9a,11a}$+$C_{9b,11b}$), 125.9 ($C_{10a,10b}$), 125.7 ($^3J_{PtC}$ = 68 Hz, $C_{4a,4b}$), 122.4 ($^4J_{PtC}$ = 9 Hz, $C_{5a,5b}$), 108.2 ($^1J_{PtC}$ = 67 Hz, $C_{1,5}$), 99.7 ($^1J_{PtC}$ = 41 Hz, $C_{2,6}$), 30.9 ($C_{4,8}$), 28.4 ($C_{3,7}$).

***cis*-[Pt(Hbph)$_2$(dmso)$_2$], 3.** Method A: **1a** (100 mg, 0.0845 mmol) was dissolved in dimethyl sulfoxide (4 mL) under continuous stirring. The solution was allowed to evaporate to dryness at 80 °C under vacuum. The solid residue was washed with diethyl ether (4 × 3 mL), dried, and then dissolved in the minimum amount of dichloromethane. Addition of 10 mL of diethyl ether and cooling to −35 °C led to the separation of 94 mg of **3** (85% yield). Method B: A solution of **2** (100 mg, 0.164 mmol) in dimethyl sulfoxide (4 mL) was stirred for 1 h, and then the solvent was removed with a rotavapor in vacuo at 80 °C. The resulting off-white solid was washed several times with diethyl ether to remove residual traces of the sulfoxide and COD, and then recrystallized from a dichloromethane/diethyl ether mixture (1/1 v/v) at −35 °C (92 mg, 85% yield). Anal. Calcd for $C_{28}H_{30}S_2O_2Pt$: C, 51.1; H, 4.6; O, 4.9; S, 9.8. Found: C, 51.3; H, 4.7; O, 5.0; S, 9.9. ^{1}H NMR ($CDCl_3$): δ 7.85 (dd, $^3J_{HH}$ = 6.6 Hz, $^4J_{HH}$ = 1.7 Hz, 4H, $H_{8a,12a}$+$H_{8b,12b}$), 7.39 (m, 4H, $H_{9a,11a}$+$H_{9b,11b}$), 7.36 (m, 2H, $H_{10a,10b}$), 7.06 (dd, $^4J_{PtH}$ = 20.3 Hz, $^3J_{HH}$ = 7.7 Hz, $^4J_{HH}$ = 1.7 Hz, 2H, $H_{6a,6b}$), 6.82 (ddd, $^3J_{HH}$ = 7.7 Hz, $^4J_{HH}$ = 1.1 Hz, 2H, $H_{5a,5b}$), 6.57 (ddd, $^4J_{PtH}$ = 13.5 Hz, $^3J_{HH}$ = 7.7 Hz, $^4J_{HH}$ = 1.7 Hz, 2H, $H_{4a,4b}$), 5.85 (dd, $^3J_{PtH}$ = 73.4 Hz, $^3J_{HH}$ = 7.7 Hz, $^4J_{HH}$ = 1.1 Hz, 2H, $H_{3a,3b}$), 3.10 (s, $^3J_{PtH}$ = 12.1 Hz, 6H, S−$(CH_3)_a$), 2.29 (s, $^3J_{PtH}$ = 16.0 Hz, 6H, S−$(CH_3)_b$). ^{13}C{^{1}H} NMR ($CDCl_3$): δ 147.1 ($^2J_{PtC}$ = 41 Hz, $C_{1a,1b}$), 146.5 ($^3J_{PtC}$ = 28 Hz, $C_{7a,7b}$), 143.5 ($^1J_{PtC}$ = 1041 Hz, $C_{2a,2b}$), 136.4 ($^2J_{PtC}$ = 26 Hz, $C_{3a,3b}$), 129.8 ($C_{8a,12a}$+$C_{8b,12b}$), 128.9 ($^3J_{PtC}$ = 57 Hz, $C_{6a,6b}$), 127.3 ($C_{9a,11a}$+$C_{9b,11b}$), 126.2 ($C_{10a,10b}$), 125.8 ($^3J_{PtC}$ = 73 Hz, $C_{4a,4b}$), 123.6 ($^4J_{PtC}$ = 11 Hz, $C_{5a,5b}$), 43.9 ($^2J_{PtC}$ = 20 Hz, S−CH_{3a}), 42.3 ($^2J_{PtC}$ = 37 Hz, S−CH_{3b}).

***cis*-[Pt(Hbph)$_2$(SEt$_2$)$_2$], 4**, was prepared and characterized in situ by bridge-splitting reaction of **1a** with an excess of SEt_2 in chloroform-*d*. ^{1}H NMR ($CDCl_3$): δ 7.96 (d, br, $^3J_{HH}$ = 7.2 Hz, 4H, $H_{8a,12a}$+$H_{8b,12b}$), 7.30 (m, br, $^3J_{HH}$ = 7.1 Hz, 4H, $H_{9a,11a}$+$H_{9b,11b}$), 7.26 (m, br, 2H, $H_{10a,10b}$), 7.03 (d, $^4J_{PtH}$ = 23.4 Hz, $^3J_{HH}$ = 7.5 Hz, 2H, $H_{6a,6b}$), 6.76 (m, 2H, $H_{5a,5b}$), 6.59 (m, $^3J_{PtH}$ = 78.8 Hz ($H_{3a,3b}$), 4H, $H_{3a,3b}$+$H_{4a,4b}$), 2.31 (m, $^3J_{PtH}$ = 25.8 Hz, $^3J_{HH}$ = 7.5 Hz, 8H, S−CH_2−CH_3), 1.13 (t, $^3J_{HH}$ = 7.5 Hz, 12H, S−CH_2−CH_3). ^{13}C{^{1}H} NMR ($CDCl_3$): δ 148.3 ($^2J_{PtC}$ = 42 Hz, $C_{1a,1b}$), 146.5 ($^1J_{PtC}$ = 1137 Hz, $C_{2a,2b}$), 146.2 ($^3J_{PtC}$ = 25 Hz, $C_{7a,7b}$), 138.1 ($^2J_{PtC}$ = 22 Hz, $C_{3a,3b}$), 130.0 ($C_{8a,12a}$+$C_{8b,12b}$), 128.4 ($^3J_{PtC}$ = 62 Hz, $C_{6a,6b}$), 126.8 ($C_{9a,11a}$+$C_{9b,11b}$), 125.3 ($C_{10a,10b}$), 125.1 ($^3J_{PtC}$ = 79 Hz, $C_{4a,4b}$), 121.7 ($^4J_{PtC}$ = 10 Hz, $C_{5a,5b}$), 27.6 (S−CH_2−CH_3), 13.1 ($^3J_{PtC}$ = 16 Hz, S−CH_2−CH_3).

[Pt(Hbph)$_2$(bpy)], 5. A dichloromethane solution (25 mL) of 2,2′-bipyridine (26.1 mg, 0.167 mmol) was added dropwise to a solution of **3** (100 mg, 0.152 mmol) in dichloromethane (25 mL). The color changed instantaneously to dark yellow. The solution was refluxed under continuous stirring for 2 h. Evaporation of most of the solvent,

(65) Kauffman, G. B.; Cowan, D. O. *Inorg. Synth.* **1960**, *6*, 211−215.
(66) Clark, H. C.; Manzer, L. E. *J. Organomet. Chem.* **1973**, *59*, 411−428.
(67) Gardner, S. A.; Gordon, H. B.; Rausch, M. D. *J. Organomet. Chem.* **1973**, *60*, 179−188.

addition of hexane, and cooling led to the separation of a dark-orange solid that was washed with hexane or Et_2O, dried, and separated out in an almost quantitative yield (95 mg, 95%). Anal. Calcd for $C_{34}H_{26}N_2Pt$: C, 62.1; H, 4.0; N, 4.3. Found: C, 61.7; H, 3.8; N, 4.0. ^{1}H NMR ($CDCl_3$): δ 8.41 (dd, $^3J_{PtH}$ = 22.6 Hz, $^3J_{HH}$ = 5.3 Hz, $^4J_{HH}$ = 1.8 Hz, 2H, $H_{6,6'}$), 7.97 (ddd, $^3J_{HH}$ = 8.0, 8.4 Hz, $^4J_{HH}$ = 1.8 Hz, 2H, $H_{4,4'}$), 7.89 (d, $^3J_{HH}$ = 8.0 Hz, 2H, $H_{3,3'}$), 7.77 (dd, $^3J_{HH}$ = 7.4 Hz, $^4J_{HH}$ = 1.7 Hz, 4H, $H_{8a,12a}$+$H_{8b,12b}$), 7.25 (ddd, $^3J_{HH}$ = 8.4, 5.3 Hz, $^4J_{HH}$ = 1.3 Hz, 2H, $H_{5,5'}$), 7.12 (dd, $^3J_{HH}$ = 7.5 Hz, $^4J_{HH}$ = 1.5 Hz, 2H, $H_{6a,6b}$), 7.05 (m, 6H, $H_{9a,11a}$+$H_{9b,11b}$+$H_{10a,10b}$), 6.87 (ddd, $^3J_{av}$ = 7.4 Hz, $^4J_{HH}$ = 1.5 Hz, 2H, $H_{5a,5b}$), 6.79 (dd, $^3J_{PtH}$ = 70.5 Hz, $^3J_{HH}$ = 7.3 Hz, $^4J_{HH}$ = 1.5 Hz, 2H, $H_{3a,3b}$), 6.71 (ddd, $^3J_{av}$ = 7.4 Hz, $^4J_{HH}$ = 1.5 Hz, 2H, $H_{4a,4b}$). ^{13}C{^{1}H} NMR ($CDCl_3$): δ 155.7 ($C_{2,2'}$), 150.1 ($C_{6,6'}$), 148.6 ($C_{1a,1b}$), 147.9 ($C_{7a,7b}$), 144.3 ($C_{2a,2b}$), 140.2 ($C_{3a,3b}$), 135.7 ($C_{4,4'}$), 130.1 ($C_{8a,12a}$+$C_{8b,12b}$), 129.9 ($C_{3,3'}$), 128.0 ($C_{6a,6b}$), 126.9 ($C_{5,5'}$), 126.4 ($C_{9a,11a}$+$C_{9b,11b}$), 125.1 ($C_{4a,4b}$), 124.6 ($C_{10a,10b}$), 121.9 ($C_{5a,5b}$).

[Pt(Hbph)$_2$(phen)], 6, was obtained from **3** and 1,10-phenanthroline following essentially the same procedure described for **5**. Anal. Calcd for $C_{36}H_{26}N_2Pt$: C, 63.4; H, 3.8; N, 4.1. Found: C, 63.4; H, 4.0; N, 4.0. ^{1}H NMR ($CDCl_3$): δ 8.68 (dd, $^3J_{PtH}$ = 21.1 Hz, $^3J_{HH}$ = 5.3 Hz, $^4J_{HH}$ = 1.2 Hz, 2H, $H_{2,9}$), 8.45 (ddd, $^3J_{HH}$ = 8.2 Hz, $^4J_{HH}$ = 1.2 Hz, 2H, $H_{4,7}$), 7.86 (s, 2H, $H_{5,6}$), 7.82 (dd, $^3J_{HH}$ = 8.2 Hz, $^4J_{HH}$ = 1.7 Hz, 4H, $H_{8a,12a}$+$H_{8b,12b}$), 7.57 (dd, $^3J_{HH}$ = 8.2, 5.3 Hz, 2H, $H_{3,8}$), 7.17 (dd, $^3J_{HH}$ = 7.5 Hz, $^4J_{HH}$ = 1.2 Hz, 2H, $H_{6a,6b}$), 6.98 (m, 6H, $H_{9a,11a}$+$H_{9b,11b}$+$H_{10a,10b}$), 6.93 (ddd, $^3J_{av}$ = 7.5 Hz, $^4J_{HH}$ = 1.2 Hz, 2H, $H_{5a,5b}$), 6.90 (dd, $^3J_{PtH}$ = 71.8 Hz, $^3J_{HH}$ = 7.5 Hz, $^4J_{HH}$ = 1.2 Hz, 2H, $H_{3a,3b}$), 6.77 (ddd, $^3J_{av}$ = 7.5 Hz, 2H, $H_{4a,4b}$). ^{13}C{^{1}H} NMR ($CDCl_3$): δ 155.6 ($C_{10',10''}$), 151.3 ($C_{4',6'}$), 150.1 ($C_{2,9}$), 148.6 ($C_{1a,1b}$), 147.9 ($C_{7a,7b}$), 144.3 ($C_{2a,2b}$), 140.1 ($C_{3a,3b}$), 135.7 ($C_{4,7}$), 130.1 ($C_{8a,12a}$+$C_{8b,12b}$), 128.0 ($C_{6a,6b}$), 126.9 ($C_{5,6}$), 126.3 ($C_{9a,11a}$+$C_{9b,11b}$), 125.4 ($C_{3,8}$), 125.1 ($C_{4a,4b}$), 124.6 ($C_{10a,10b}$), 121.5 ($C_{5a,5b}$).

Instrumentation and Measurements. NMR analyses were performed on a Bruker AMX-R 300 spectrometer equipped with a broadband probe operating at 300.13 and 75.46 MHz for ^{1}H and ^{13}C nuclei, respectively. ^{1}H and ^{13}C NMR chemical shifts are reported in ppm (δ) with respect to TMS and referenced to the residual protiated impurities of the deuterated solvent. Coupling constants are given in hertz. Usually samples were degassed prior to use by freeze-pump methodology. The temperature within the probe was checked using the methanol method.[68] 2D-COSY experiments were performed in a phase-sensitive mode. Normal-range ^{13}C,^{1}H-correlation experiments (HMQC, heteronuclear multiple quantum coherence) were recorded by a standard inverse detection sequence considering $^1J_{CH}$ = 145 Hz. Relaxation times T_1 for protons were set at 0.55 s (**1**), 0.9 s (**4**−**6**), and 0.85 s (**3**). Phase-sensitive ^{1}H 2D-NOESY experiments were performed with a standard pulse sequence by using a mixing time of 0.8 s (**3**, **6**) or 0.6 s (**1**). UV−vis spectra were run with a rapid-scanning Hewlett-Packard model 8452A spectrophotometer or with a Perkin-Elmer Lambda3 spectrophotometer, interfaced with a microcomputer for data collection and equipped with a cell compartment thermostated by a Perkin-Elmer PTP (Peltier temperature programmer). The temperature accuracy was ±0.05 °C.

Crystallography. Crystals of **5** and **6**, suitable for X-ray diffraction, were obtained by slow diffusion of hexane into a concentrated toluene solution and are air stable. Crystals of **5** were mounted on an CAD4 diffractometer for the unit cell and space group determinations and for the data collection. The unit cell constants, space group determination, and the data collection for **6** were carried out, at 200(2) K, on a Bruker SMART diffractometer equipped with a CCD detector.

Structural Study of [Pt(Hbph)$_2$(bpy)], 5. Data were measured with variable scan speed to ensure constant statistical precision on the collected intensities. Three standard reflections were used to check the stability of the crystals and of the experimental conditions and were measured every hour. The collected intensities were corrected for Lorentz and polarization factors.[69] An empirical absorption correction[70] was also applied by using azimuthal (Ψ) scans of three "high-χ" ($\chi \geq 80°$) reflections. Of the 3487 independent data collected, 2076 were considered as observed and used for the solution and refinement of the structure. Selected crystallographic and other relevant data are listed in Table 1 and in Table S1 of the Supporting Information. The standard deviations on intensities were calculated in term of statistics alone. The structure was solved by direct and Fourier methods and refined by full matrix least-squares[71] (the function minimized being $[\sum w(F_o^2 - (1/k)F_c^2)^2]$) using anisotropic displacement parameters for all atoms. No extinction correction was deemed to be necessary. The contribution of the hydrogen atoms in their calculated positions [C−H = 0.95 (Å), B(H) = 1.3−1.5 × B(C_{bonded}) (Å^2)] was included in the refinement using a riding model. Upon convergence (see Table S1), no significant features were found in the Fourier difference map. All calculations were carried out by using the PC version of the SHELX-97 and ORTEP programs.[71] The scattering factors used, corrected for the real and imaginary parts of the anomalous dispersion, were taken from the literature.[72]

Structural Study of [Pt(Hbph)$_2$(phen)]·(C_7H_8), 6·(C_7H_8). The crystal was cooled to 200(2) K, and the space group was determined from the systematic absences; the cell constants were refined, at the end of the data collection, using the data reduction software SAINT.[73] Data were collected by using an ω scan in steps of 0.3°; a list of experimental conditions for the data collection is given in Table S1. The collected intensities were corrected for Lorentz and polarization factors and empirically for absorption using the SADABS program.[74] Selected crystallographic and other relevant data are listed in Table 1 and in the Supporting Information Table S1. The standard deviations on intensities were calculated in term of statistics alone as shown in Tables 1 and S1. The structure was solved by Patterson and Fourier methods and refined by full matrix least-squares,[71] minimizing the function $[\sum w(F_o^2 - (1/k)F_c^2)^2]$ and using anisotropic displacement parameters for all atoms. No extinction correction was deemed necessary. Toward the end of the refinement, a clathrated toluene molecule was found on a difference Fourier map. This molecule is highly disordered, and therefore the refined geometry is only approximate; however, this disorder is not affecting the refined geometry of the complex. The contribution of the hydrogen atoms in their calculated positions [C−H = 0.95(Å), B(H) = 1.3−1.5 × B(C_{bonded}) (Å^2)] was included in the refinement using a riding model. The handedness of the structure was tested by refining the Flack's parameter.[75] Upon convergence, the final Fourier difference map showed no significant peaks. All calculations were carried out, as above, using the PC version of the SHELX-97 programs.[71]

Computational Details. Molecular mechanics calculations were performed on a Pentium IV personal computer using the Spartan package version '02.[76] A modified version of the MMFF94 force field implemented for transition metal parameters was used in the minimization calculations. The X-ray structure of [Pt_2(*p*-tol)$_4$(μ-SEt_2)$_2$],[42] imported from the Cambridge Crystallographic Database (CSD), was properly modified and used as input for the calculations to gauge the performance of the MMFF calculations. Different lowest-energy conformations of the dinuclear complex **1** were generated by the

(68) (a) Van Geet, A. L. *Anal. Chem.* **1968**, *40*, 2227−2229. (b) Van Geet, A. L. *Anal. Chem.* **1970**, *42*, 679−680.

(69) *MolEN: Molecular Structure Solution Procedure*; Enraf-Nonius: Delft, The Netherlands, 1990.
(70) North, A. C. T.; Phillips, D. C.; Mathews, F. S. *Acta Crystallogr.* **1968**, *A24*, 351−359.
(71) Sheldrick, G. M. *SHELX-97. Structure Solution and Refinement Package*; Universität Göttingen, 1997. Farrugia, L. J. *J. Appl. Crystallogr.* **1997**, *30*, 565.
(72) *International Tables for X-ray Crystallography*; Kynoch: Birmingham, England, 1974; Vol. IV.
(73) *SAINT: SAX Area Detector Integration*; Siemens Analytical Instrumentation, 1996.
(74) Sheldrick, G. M. *SADABS*; Universität Göttingen: Göttingen, Germany, 1996.
(75) Flack, H. D. *Acta Crystallogr.* **1983**, *A39*, 876−881.
(76) Spartan '02, Wavefunction, Inc., Irvine, CA.

systematic variation of the dihedral angles S−Pt−C2−C1 and C2−C1−C7−C8 for all four Hbph fragments. Full geometry optimization for each structure to a gradient convergence limit of less than 10^{-5} was carried out before a final single point energy calculation. During the minimization, no symmetry restriction was imposed, but the positions of all atoms in both of the square coordination planes, that is, Pt−S1−S2−C2a−C2b, were kept frozen.

Kinetic Studies. (a) Spectrophotometric Kinetics. Nucleophilic substitution reactions of **3** with bpy and phen to yield **5** and **6** were carried out at 298.2 ± 0.05 K in toluene as the solvent and were followed by repetitive scanning of the spectrum at suitable times in the wavelength range 380−540 nm or, at fixed wavelength, where the absorbance of the starting sulfoxide complex is negligible in comparison to that of the final diimine product [Pt → (N−N) MLCT] band at λ_{max} = 484 nm, **5**; 478 nm, **6**. The reactions, carried out in the presence of at least a 10-fold excess of chelating ligand and a 20-fold excess of dmso over the complex, went to completion with the final spectra being identical to those of authentic samples of [Pt(Hbph)$_2$(N−N)]. Abstract factor analysis[77] of the spectral changes confirmed that the diimine-containing product is the only absorbing species in solution, and there was no indication of the presence of significant amounts of any intermediate species. Rate constants, k_{obsd}/s^{-1}, were evaluated by using the SCIENTIST software package,[46] from nonlinear least-squares fits of the experimental data to the equation $A_t = A_\infty + (A_0 - A_\infty)\exp(-k_{obsd}t)$, with A_0, A_∞, and k_{obsd} as the parameters to be optimized (A_0 = absorbance after mixing of reagents, A_∞ = absorbance at completion of reaction), and are collected in Tables S3 and S4 of the Supporting Information, as a function of the nucleophile (N−N) and nucleofuge (dmso) concentrations.

(b) Magnetization Transfer Experiments. The rate constants for the moderately fast exchange of dmso between two nonequivalent sites, S_{bound} and S_{free}, in complex **3**, were determined as a function of both temperature and added sulfoxide concentration by magnetization transfer experiments, as described by Forsèn−Hoffman.[78] In a typical experiment, the resonance of the free site, S_{free} (at δ 2.6), in $CDCl_3$ was completely saturated through a selective rf pulse, while the resonance of S_{bound} (at δ 3.1) was monitored as a function of the variable irradiation time. Thus, the condition of a good separation of the signals of free and bound ligands was fulfilled, allowing saturation of the free signal without perturbing the magnetization of the other signal. The integrals of S_{bound} (M_b) were fitted by linear regression analysis to eq 11

$$\ln[(M_b)_t - (M_b)_\infty] = -\ln(M_b)_0(\tau_{1b}/\tau_b) + t/\tau_{1b} \quad (11)$$

where $(M_b)_0$, $(M_b)_t$, and $(M_b)_\infty$ are the integrals of the peak before saturation, at the time t, and after a prolonged saturation, respectively. τ_{1b} is correlated to T_{1b}, the spin−lattice relaxation time, and to τ_b, the lifetime of the observed site, by eqs 12−13.

$$(M_b)_\infty = (M_b)_0(\tau_{1b}/T_{1b}) \quad (12)$$

$$1/\tau_{1b} = 1/\tau_b + 1/T_{1b} \quad (13)$$

The pseudo-first-order constants were calculated as $k_{exch} = 2\tau_b^{-1}$, taking into account the fact that the exchange involves two equivalent sites. All of the rates of ligand exchange were independent of the concentration of free sulfoxide. The rate constants at different temperatures from magnetization transfer experiments (in Supporting Information Table S6) were fitted to the Eyring equation

$$k = (kT/h)\exp(-\Delta H^{\ddagger}/RT)\exp(\Delta S^{\ddagger}/R) \quad (14)$$

leading to the activation parameters reported in Table S6.

Acknowledgment. We thank the Ministero dell'Istruzione, dell'Università e della Ricerca (MIUR), Programmi di Ricerca Scientifica di Rilevante Interesse Nazionale, Cofinanziamento 2002-2003, the Università degli Studi di Messina, and CNR for funding this work.

Supporting Information Available: Text giving experimental details and a full listing of crystallographic data for **5** and **6-(C_7H_8)** (CIF), including tables of positional and isotropic equivalent displacement parameters, calculated positions of the hydrogen atoms, anisotropic displacement parameters, bond distances, and bond and torsion angles. ORTEP figures showing the full numbering schemes are also included. Table of NOESY connectivities for **1a** and **1b**. Tables giving the concentration and temperature dependencies of primary kinetic data. A figure showing experimental and calculated isotopic distribution of $(M - C_{12}H_9 - C_2H_5 + H)^+$ for **1a**. This material is available free of charge via the Internet at http://pubs.acs.org.

JA030486U

(77) (a) Uguagliati, P.; Benedetti, A.; Enzo, S.; Schiffini, L. *Comput. Chem.* **1984**, *8*, 161−168. (b) Sandrini, P. L.; Mantovani, A.; Crociani, B.; Uguagliati, P. *Inorg. Chim. Acta* **1981**, *51*, 71−80. (c) Malinowski, E. R.; Hovery, D. G. *Factor Analysis in Chemistry*; Wiley-Interscience: New York, 1980; pp 159−161.

(78) Forsèn, S.; Hoffmann, R. A. *J. Chem. Phys.* **1963**, *39*, 2892−2901.